AD-A046 275 NATIONAL OCEANIC AND ATMOSPHERIC ADMINISTRATION BOUL--ETC F/G 4/2
REMOTE SENSING WIND AND WIND SHEAR SYSTEM.(U)
MAR 77 P A MANDICS

UNCLASSIFIED FAA-RD-77-54 DOT-FA72WAI-281 NL

| OF |
AD A046275

END
DATE FILMED
12-77
DDC

Report No. FAA-RD-77-54

REMOTE SENSING WIND AND WIND SHEAR SYSTEM

Peter A. Mandics
Wave Propagation Laboratory
Environmental Research Laboratories
National Oceanic and Atmospheric Administration
Boulder, Colorado 80302

March 1977
Interim Report

Document is available to the U.S. public through the National Technical Information Service, Springfield, Virginia 22161.

Prepared for

U.S. DEPARTMENT OF TRANSPORTATION
FEDERAL AVIATION ADMINISTRATION
Systems Research & Development Service
Washington, D.C. 20590

NOTICE

This document is disseminated under the sponsorship of the Department of Transportation in the interest of information exchange. The United States Government assumes no liability for its contents or use thereof.

Technical Report Documentation Page

1. Report No.	2. Government Accession No.	3. Recipient's Catalog No.
FAA-RD-77-54		

4. Title and Subtitle
REMOTE SENSING WIND AND WIND SHEAR SYSTEM

5. Report Date
March 1977

6. Performing Organization Code
NOAA/ERL WPL R45x2

8. Performing Organization Report No.
35p.

7. Author(s)
Peter A. Mandics

9. Performing Organization Name and Address
Wave Propagation Laboratory
Environmental Research Laboratories
National Oceanic and Atmospheric Administration
Boulder, Colorado 80302

10. Work Unit No. (TRAIS)

11. Contract or Grant No.
DOT-FA72WAI-281

13. Type of Report and Period Covered
Interim Report covering Phase III for period January 1974 – September 1976

12. Sponsoring Agency Name and Address
Federal Aviation Administration
System Research and Development Service
Airports Division, Aviation Weather Systems Branch
Washington, D. C. 20591

14. Sponsoring Agency Code
FAA/ARD-450 on Phase 3

15. Supplementary Notes

16. Abstract

The prototype development of an acoustic Doppler remote-sensing system to detect low-level wind shear generated by synoptic-scale features such as frontal surfaces is described. The detector system measures the vertical profile of wind by determining the Doppler frequency shift of vertically transmitted acoustic signals that are scattered by small-scale atmospheric inhomogeneities. Following earlier acoustic Doppler tests at Stapleton International Airport in Denver, Colorado, significant improvements have been accomplished on the acoustic transmitter and receiver antennas, and signal processing. A conical horn reflector antenna with a 2-m diameter aperture fed by 12 high-power acoustic drivers through a manifold increased the transmitted power by more than 100%. Substantial improvements have been achieved in received signal-to-noise ratio by developing a narrow-beam, off-focus steered receiving antenna that is capable of tracking the upward propagating acoustic pulse. Development of new system software made all-digital signal processing and computerized system control possible. Tests of one leg of the prototype at Table Mountain near Boulder, Colorado revealed that the system measured winds reliably up to a height of 600 m when surface winds did not exceed 10 m s^{-1}. The deleterious effects of precipitation on system performance have not been fully evaluated yet. A brief review of wind-shear types and their detection is followed by a discussion of second-generation wind-shear detection systems employing lidar and microwave radar devices.

17. Key Words	18. Distribution Statement
Acoustic Doppler; Wind Shear; Wind Profile Measurement; Remote Sensing.	Document is available to the U.S. public through the National Technical Information Service, Springfield, Virginia 22161

19. Security Classif. (of this report)	20. Security Classif. (of this page)	21. No. of Pages	22. Price
Unclassified	Unclassified	34	

Form DOT F 1700.7 (8-72) Reproduction of completed page authorized

406292

METRIC CONVERSION FACTORS

Approximate Conversions to Metric Measures

Symbol	When You Know	Multiply by	To Find	Symbol
	LENGTH			
in	inches	*2.5	centimeters	cm
ft	feet	30	centimeters	cm
yd	yards	0.9	meters	m
mi	miles	1.6	kilometers	km
	AREA			
in^2	square inches	6.5	square centimeters	cm^2
ft^2	square feet	0.09	square meters	m^2
yd^2	square yards	0.8	square meters	m^2
mi^2	square miles	2.6	square kilometers	km^2
	acres	0.4	hectares	ha
	MASS (weight)			
oz	ounces	28	grams	g
lb	pounds	0.45	kilograms	kg
	short tons (2000 lb)	0.9	tonnes	t
	VOLUME			
tsp	teaspoons	5	milliliters	ml
Tbsp	tablespoons	15	milliliters	ml
fl oz	fluid ounces	30	milliliters	ml
c	cups	0.24	liters	l
pt	pints	0.47	liters	l
qt	quarts	0.95	liters	l
gal	gallons	3.8	liters	l
ft^3	cubic feet	0.03	cubic meters	m^3
yd^3	cubic yards	0.76	cubic meters	m^3
	TEMPERATURE (exact)			
°F	Fahrenheit temperature	5/9 (after subtracting 32)	Celsius temperature	°C

*1 in = 2.54 (exactly). For other exact conversions and more detailed tables, see NBS Misc. Publ. 286, Units of Weights and Measures, Price $2.25, SD Catalog No. C13.10:286.

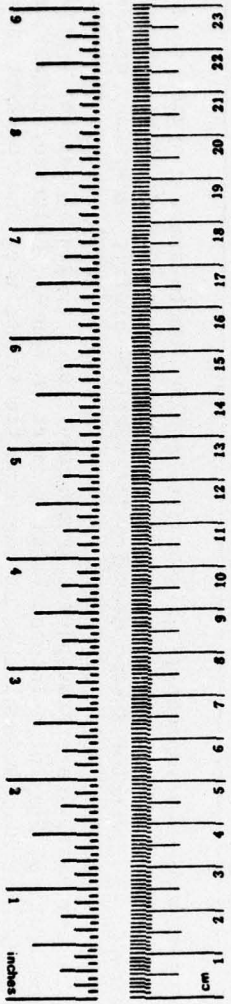

Approximate Conversions from Metric Measures

Symbol	When You Know	Multiply by	To Find	Symbol
	LENGTH			
mm	millimeters	0.04	inches	in
cm	centimeters	0.4	*inches*	*in*
m	meters	3.3	feet	ft
m	meters	1.1	yards	yd
km	kilometers	0.6	miles	mi
	AREA			
cm^2	square centimeters	0.16	square inches	in^2
m^2	square meters	1.2	square yards	yd^2
km^2	square kilometers	0.4	square miles	mi^2
ha	hectares (10,000 m^2)	2.5	acres	
	MASS (weight)			
g	grams	0.035	ounces	oz
kg	kilograms	2.2	pounds	lb
t	tonnes (1000 kg)	1.1	short tons	
	VOLUME			
ml	milliliters	0.03	fluid ounces	fl oz
l	liters	2.1	pints	pt
l	liters	1.06	quarts	qt
l	*liters*	0.26	gallons	gal
m^3	cubic meters	35	cubic feet	ft^3
m^3	cubic meters	1.3	cubic yards	yd^3
	TEMPERATURE (exact)			
°C	Celsius temperature	9/5 (then add 32)	Fahrenheit temperature	°F

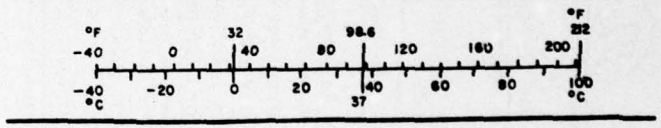

PREFACE

Phase III of the remote sensing wind and wind-shear system effort has been performed under the direction of Dr. D. W. Beran. The dedicated and conscientious work of many individuals in the Remote Sensor Applications Program Area and other groups within the Wave Propagation Laboratory insured the success of the project. J. T. Priestley designed and tested the array transmitter antenna. He was ably assisted by L. A. Vohs. B. C. Willmarth developed a unique new technique for measuring acoustic antenna beam patterns and performed these measurements in collaboration with M. Spowart and F. Mottola. B. N. Nagarkar and Dr. R. D. Finch, Applied Acoustics Corporation, Houston, Texas performed the crucial model study of the receiver antenna. R. J. Keeler, D. E. Hunter, R. M. Hardesty, G. Lopez, L. Rodda, and K. B. Young designed, developed, and tested the sophisticated new computer software package. E. J. Owens, R. W. Krinks, M. Bottomley, C. E. Case, and D. Sipple were responsible for the extensive redesign and implementation of the analog and digital circuitry. J. F. Pratte evaluated the performance of the Table Mountain prototype. Last, but not least, J. S. Alspaugh ably took care of the many administrative tasks associated with the project.

TABLE OF CONTENTS

TABLE OF CONTENTS (continued)

LIST OF ILLUSTRATIONS

LIST OF ILLUSTRATIONS (continued)

LIST OF TABLES

REMOTE SENSING WIND AND WIND SHEAR SYSTEM

1. INTRODUCTION

The Phase I and II report for this project (Beran, 1974) described an early wind-shear detection experiment at Stapleton International Airport in Denver, Colorado. The detection system was based on the acoustic Doppler technique and was the forerunner of the systems described in this report. Results from the Stapleton work guided most of the activity during Phase III.

Wind-shear-related aircraft accidents during Phase III added to the urgency of the detector development program and provided impetus for an accelerated work schedule which called for the installation of the first operational test system while engineering development work on the prototype was still under way. Analysis of the meteorological conditions associated with these accidents also indicated that single, vertically profiling devices like acoustic Doppler and VAD scanning CW lasers might not be totally effective in detecting the more capricious thunderstorm-related wind shear.

The [illegible]el work effort mentioned above was [illegible] with the full realization that the [illegible]rational test device could be outmoded [illegible] it was installed by ongoing engineering [illegible]pment and work on second-generation systems. It was assumed that the preliminary acoustic Doppler design would hold firm through the final field tests and that no second-generation breakthrough would occur.

However, a major breakthrough in microwave radar technology did occur during this phase of the project. It was demonstrated that through the use of new processing techniques EM radar could be used to measure winds in the clear air as well as in precipitation. While this radar is still in the early research stage, it is of vital importance to the future direction of wind-shear detection system development. The new radar development could conceivably provide an all-weather alternative to the acoustic/radar system described in this report.

2. STAPLETON ACOUSTIC DOPPLER TESTS

2.1 Background

During the latter portion of 1973, an experimental version of the acoustic wind-shear detection system was installed and operated for three months at Stapleton International Airport in Denver, Colorado. The goals of these tests were to determine the feasibility of operating an acoustic device at a major airport, and to identify system components which would require further engineering development.

2.2 System Description

The Stapleton system was fully described in the Final Phase I and II Report (Beran, 1974). Suffice to say here that it was a two-legged system with a single vertically pointed transmitter and two smaller transmitters near the receivers along each of the legs. Figure 1 shows an artist's concept of the configuration with its fan beam patterns, and Figure 2 shows a block diagram of the major system components.

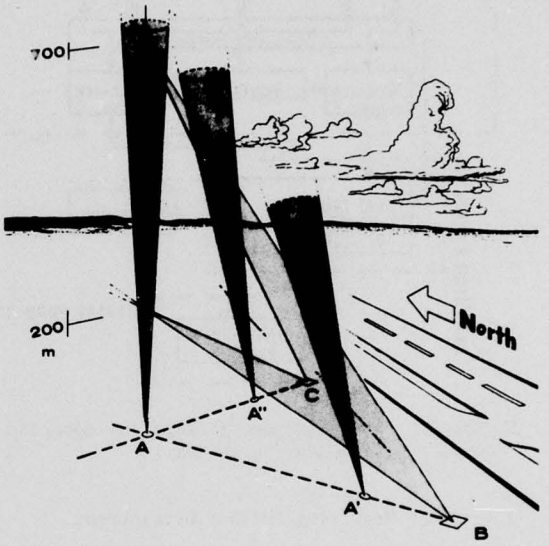

Figure 1. View of the multi-transmitter, multi-receiver Stapleton acoustic Doppler wind-measuring system.

2.3 Major Difficulties

One major difficulty with testing a device which measures a wind profile to several hundred meters above the ground, especially at an active airport, is the lack of acceptable standard sensors for making comparison measurements. At Stapleton, wind data were available only from radiosondes launched twice a day some 3 miles away. When the temperamental experimental equipment used at Stapleton was operating properly, good agreement was found between the radiosonde data and the acoustic Doppler winds. The day-to-day performance of the system was judged by observing the down time and the signal-to-noise ratio during operating periods. This procedure demonstrated that an acoustic system could be operated in the noisy airport environment, however, a number of system modifications and component design improvements were needed prior to reaching the prototype stage. Areas that were identified as requiring further development are listed below:

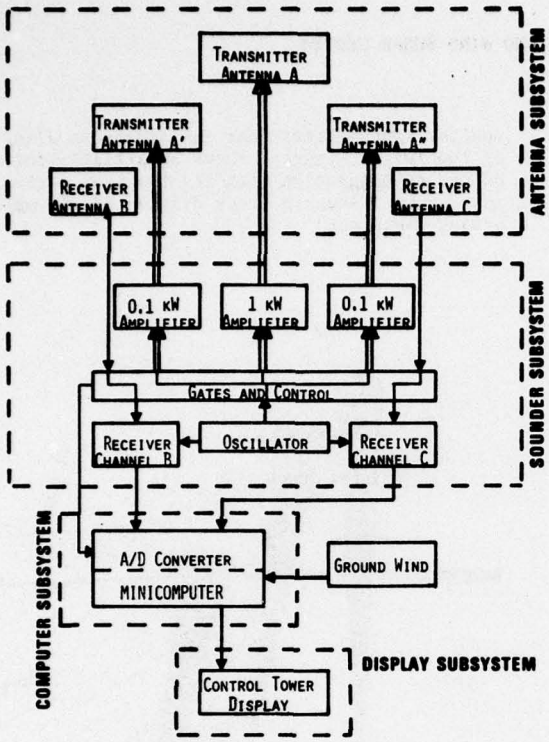

Figure 2. Block diagram of Stapleton acoustic Doppler wind-measuring system.

2.4 Areas Requiring Further Development

2.4.1 Antenna Sidelobes

The main transmitter used at Stapleton was a 3 m diameter parabolic dish fed by four 100 Watt acoustic drivers positioned at the focal point of the parabola. Analysis of the transmitter beam pattern and its intersection with the receiver beam showed that excessively strong sidelobes could create a serious error in the wind readings because the scattering volume was not always along the axis of the transmitted beam. It became clear that reduced sidelobes would produce a significant improvement in the accuracy of wind measurements.

2.4.2 Signal-to-Noise Ratio

Basic to any system is its overall signal-to-noise ratio. One obvious way to improve this ratio is to transmit higher acoustic power. This was difficult to do at Stapleton, because the acoustic transducers were being driven near their capacity and the addition of more transducers or a different type of sound source would have involved a major redesign. Increasing the transmitted power remained a worthwhile goal, however, and it became one of the design objectives during the Phase III work.

2.4.3 Transmitter Efficiency

The transmitter efficiency, the ratio of electrical power input to acoustic power output, at Stapleton was also judged to be poor. Improvements here, as in Section 2.4.2, would result in a better signal-to-noise ratio.

2.4.4 Receiver Design

At Stapleton, it was assumed that the receiver beams were fanned, or at least, wide enough to cover the vertical extent of the profile. Later analysis showed that while they were wide enough, the reduction in sensitivity near their edges was sufficient to cause serious signal loss. This, and the fact that the fan beam has an inherently poor signal-to-noise ratio indicated the need for extensive redesign of the receiving antenna and transducers.

2.4.5 Ambient Acoustic Noise

The need to protect the receiver antenna and transducers from the ambient noise field was amplified by the Stapleton tests. The crude bunkers were adequate only for experimental work and the need for an improved prototype design became clear. In addition, information on the interaction between the protective bunker and the antenna was required.

Critical questions concerning the effective receiver aperture of a bunker-enclosed antenna, and the type of acoustic treatment that the bunker would need were still unanswered.

2.4.6 Software Requirements

The analog Doppler extraction technique incorporated into the receiver electronics for the Stapleton tests proved to be less than perfect and was responsible for an observed underestimate in measured winds, as well as inaccuracies near zero wind speeds. This problem could be solved by introducing computer software for processing the complete frequency spectra and shifting the Doppler extraction from the analog to the digital portions of the system. The spectral technique also provides an additional 10 dB improvement in signal-to-noise ratio.

2.4.7 Site Selection

The importance of selecting proper sites for the receiver antennas was clearly demonstrated at Stapleton. The site, near the north end of the north-south runway, was selected for maximum exposure to the noise from arriving and departing airborne aircraft. It was learned that far greater interference was caused by the long line of taxiing aircraft (as many as 8 or 9 at a time) lining up for takeoff. Such problems can be avoided by conducting careful preliminary noise survey of the proposed site.

2.4.8 Beam Pattern Measurements

The need for improved receiver and transmitter beam patterns was mentioned above. Our success in making improvements in this area could be judged only by performing actual measurements of the antenna beam patterns after they were placed in their final housing. Because of the size of the antenna structures and the need to make far-field measurements, this proved to be a very difficult problem which was resolved only after considerable development effort.

2.5 Summary

It was clear at the outset of Phase III that, although the concept of acoustic Doppler wind measurements remained valid, major improvements in the system were needed before engineering specifications for an operational model could be generated. The goal of Phase III was the accomplishment of these improvements and the installation of a modified system at the Table Mountain field site near Boulder, Colorado where the new components could be tested as part of a prototype system. The Eastern Air Lines Flight 66 accident at JFK Airport in New York on June 24, 1975 had a decided impact on the project schedule and was a major factor in the acceleration of Phase III. In addition, Phase IV calling for the installation of an operational first system, was rescheduled to take place in parallel with the prototype testing at Table Mountain. The next section describes the development work leading up to the Table Mountain prototype installation and testing.

3. PHASE III ENGINEERING DEVELOPMENT

3.1 Transmitter Redesign

As described in Section 2, increased power output and reduction in the antenna sidelobe levels were the most important goals of the main transmitter redesign effort. We concluded that our approach was nearing the limits of acoustic transmitter state-of-the-art and that further basic research was required before we could realize a substantially improved design. Further theoretical analysis indicated two possible solutions to the transmitter redesign problem.

3.1.1 First Solution to Transmitter Redesign

3.1.1.1 Amplitude-Shaded Square Array Antenna

One of the most attractive potential solutions was the use of an amplitude-shaded square array of acoustic transducers for the main transmitter. Computer simulations demonstrated that a beam pattern similar to that shown on the right side of Figure 3 could be produced. This pattern can be compared with the one shown on the left of Figure 3, which is the theoretical pattern for the 3 m parabolic dish used at Stapleton. The anticipated sidelobe improvement is obvious and the slight broadening of the main beam was judged to be acceptable.

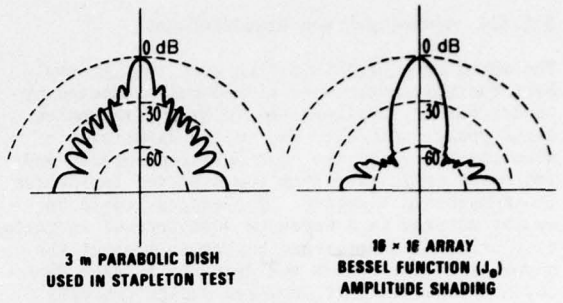

Figure 3. Theoretical beam patterns for parabolic dish antenna used at Stapleton and experimental amplitude-shaded array.

3.1.1.2 Impedance Matching

A parallel development effort to find ways of improving the acoustic impedance matching between the driver and the air resulted in a second new concept which could be incorporated into the array transmitter design. For discrete frequencies, it is possible to improve the acoustic coupling with the atmosphere by replacing the familiar broadband exponential horn with a resonant tuned coupler. These couplers consist of a cylindrical tube having a length and diameter matched to the operating frequency. This resonant cylinder is attached to the driver by a second tube with a diameter which matches the driver opening.

3.1.1.3 Theoretical Refinements

Theoretically these tuned resonant couplers could be inverted and used as the elements of an array. By doing this we envisioned a transmitter antenna array like that shown in Figure 4. The inset illustrates the inverted resonant coupler and the driver connected by a smaller tube running through the concrete roof of the enclosure protecting the drivers. The inverted coupler would prevent precipitation from entering the driver and the bunker roof would provide a reflecting backplane for the array of couplers.

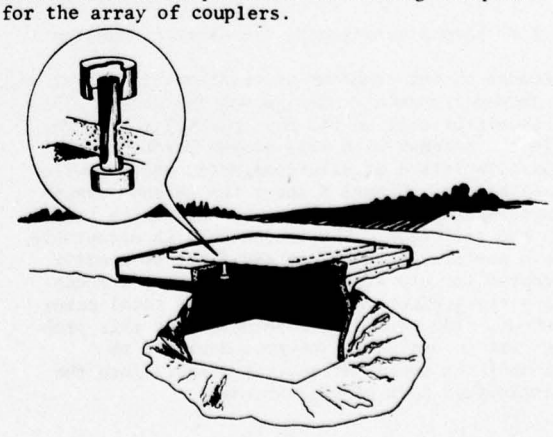

Figure 4. View of weatherproof tuned resonant coupler array.

3.1.1.4 Advantages and Disadvantages

The advantages of this design were that it would have the well-controlled sideblobes predicted by theory for an amplitude-shaded array, increased input power capability due to the dispersion of acoustic energy to the numerous transducers, and increased efficiency from the expected improvement in atmospheric coupling. The concept could be easily adapted to a hardened weatherproof installation using an underground bunker to protect the supporting electronics and drivers. A major disadvantage was that it involved design concepts which were ahead of the acoustic transmitter state-of-the-art. Phased arrays had been proven at much higher frequencies for underwater applications and the resonant tuned coupler had been successfully applied to fog horns. We did not know how well these concepts would work when the coupler was inverted and incorporated into a low-frequency array antenna for use in the atmosphere.

3.1.1.5 Prototype Array Construction

Following theoretical studies and computer simulations, the construction of a prototype array antenna was started. The prototype was to be made up of a very rigid but transportable backplane supporting the drivers and resonant couplers. Development of the couplers proceeded in parallel with the backplane construction. Appendix A contains details related to the coupler design. The array development was carried out in stages with thorough testing of individual components. Preliminary results were encouraging and major problems did not arise until the backplane-mounted coupler interactions were tested. It was found that these interactions were much higher than expected and would have been very difficult to control. In addition, factors such as atmospherically induced differential heating of the backplane and the resultant temperature gradients were severe enough to cause considerable distortions in the expected beam pattern. Some of these problems could be solved in a research setting, but they would have added an unacceptable maintenance burden for an operational transmitter. Because of this, further array research was abandoned.

3.1.2 Second Solution to Transmitter Redesign

Because of the problems associated with the array, a second transmitter design was initiated. This transmitter used an off-axis parabolic horn reflector antenna with well-proven performance characteristics at electromagnetic and acoustic wavelengths. Figure 5 shows the antenna shape superimposed on a parabolic surface which serves as the reflector. The antenna had an acceptable beam pattern, however, it could not be readily adapted for use with multiple drivers, a necessary arrangement for increasing the total power output. The most direct solution for this problem was to design an acoustic manifold to channel the output of several drivers into the single feed port of the antenna.

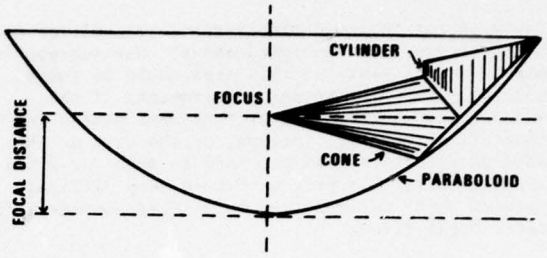

Figure 5. Off-axis parabolic horn antenna shown with the parabolic section from which it is derived.

3.1.2.1 Multiple-Feed, Off-Axis, Parabolic Horn Reflector Antenna

A photograph of the prototype off-axis transmitter, complete with manifold and amplifier housing, is shown in Figure 6. The manifold contained in the housing is illustrated in Figure 7. This unit was designed to accommodate twelve 100 Watt (electrical) transducers and was mounted at the apex of the cone which illuminates the parabolic surface. Tests of this unit showed that its overall efficiency was disappointingly low, but that it provided a significant power increase over that of the Stapleton system. The low efficiency was attributed to acoustic non-linearities generated in the manifold and a second test unit was designed with the objective of reducing these effects. A detailed report on the manifold development and testing effort is contained in Appendix B. While the second manifold is more compact and aesthetically pleasing, its efficiency was little different from that of the first model. Other potential transmitter improvements were identified during the development work (see Appendix B), and were incorporated into the prototype transmitter.

In summary, the best operational transmitter of those tested was judged to be the multiple-feed off-axis parabolic horn. For optimum sidelobe reduction the exit aperture should be fitted with a shielding cuff and some of the internal surfaces of the antenna should be lined with absorbing material (see Kurze et al., 1975).

3.2 Receiver Redesign

A second major development effort during Phase III involved the receiver antenna and bunker. It has been mentioned in Section 2 that the fan beam used at Stapleton was unacceptable and that the protective bunker required significant design changes.

3.2.1 Receiver Improvement Considerations

Two methods of improving the receiver antenna were investigated. One was to produce a narrow receiver beam and to steer it, as described below,

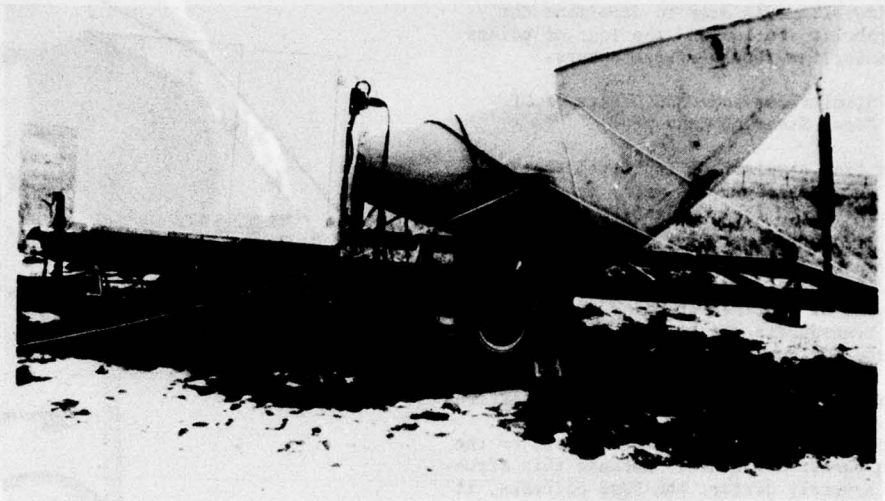

Figure 6. Transmitter unit with off-axis parabolic horn antenna and amplifier housing.

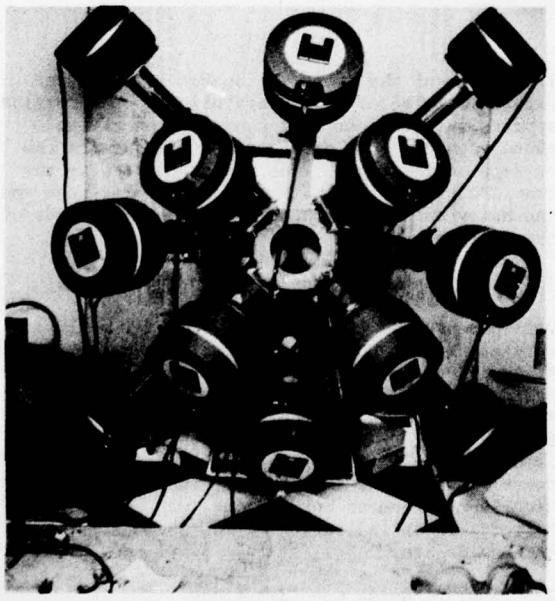

Figure 7. Multiple-feed antenna manifold with transducers attached located inside amplifier housing.

along the axis of the main transmitter so that the transmitted acoustic pulse could be tracked as it travelled upward. The second was to interchange the receiver and transmitter positions and use a single vertically pointed receiver beam with fanned or steered transmitter beams. Recognizing that rain noise was a problem it was thought to be unwise to contemplate a vertically pointed receiver which would have maximized the exposure to rain. In addition, the steered transmitter would have posed severe switching problems and a fanned transmitter would have been very inefficient.

3.2.2 Beam Steering Methods

Two receiver beam steering methods appeared to have promise; one, a phased array of transducers which could be electronically adjusted to steer the beam (as is done with EM phased arrays) and, the second, a simple parabolic antenna with transducers placed at off-focus positions to produce the desired beam directions.

3.2.2.1 Phased-Array Concept

Some of the results of the transmitter array work were equally applicable to the receiver. Because of the system complexity and maintenance problems that were potentially too severe for an operational system, the phased array receiver concept was eliminated from consideration.

3.2.2.2 Off-Focus Steering Concept

The off-focus steering concept, a technique that had already been used with acoustic antennas, was judged to have the greatest promise for producing a steerable receiver beam. Because off-axis parabolic antennas have the significant advantage

of no beam blockage by transducers, this aspect was also incorporated as a desirable design goal. Computer simulation was used to determine the optimum parabolic section and the loci of points for positioning the receiver transducers.

3.2.2.2.1 Simulations and Model Tests of Off-Focus Steering Concept

The results from simulations indicated that an elliptical section centered 1 meter from the y axis and 1.75 m from the x axis of a parabola defined by $(x^2 + y^2) = 8\ (z-2)$ would be optimum. It was also determined that seven transducer positions would be sufficient for producing the desired amount of vertical steering. Additional columns of transducers parallel to the first one could be used for horizontal steering.

While it was possible to predict the beam patterns of a free-standing antenna and transducer, we could not determine accurately the effects of the surrounding bunker structure. Because this structure could severely distort the beam patterns, it was essential that its effects be carefully assessed before a full-scale prototype was constructed. The least expensive method of doing this was to construct a scale model of the bunker and antenna, and to perform beam pattern measurements in an anechoic chamber. This was accomplished by Dr. Finch at the University of Houston, Houston, Texas under a subcontract. The details of this work are described by Nagarkar and Finch (1975). These tests demonstrated that the bunker did affect the antenna beam patterns, but that the detrimental effects could be reduced or eliminated by lining the inside bunker surfaces with sound absorbing material. It was concluded that the bunker should act, as near as possible, as an acoustic black body. The anechoic chamber tests showed that this could be accomplished to a large extent by lining only one wall (opposite to the transducers) with sound absorbing material.

3.2.2.2.2 Prototype Receiver Antenna

Following the scale model anechoic chamber tests, a full-sized version of the receiver bunker was constructed at the Table Mountain field site. Figure 8 shows a cutaway view of the prototype bunker. The acoustic absorbing liner was constructed from aluminum honeycomb panels cut and backed such that the honeycomb cells created varying path lengths which provided broadband acoustic absorption characteristics (Wirt, 1973).

The Table Mountain prototype bunker installation is shown in Figure 9. The area surrounding the bunker was backfilled and graded to eliminate any sharp terrain discontinuities which could generate beam distorting wind eddies and wind noise. The bunker opening was covered with an acoustically transparent, open-cell foam supported by a steel gridwork. The foam cover significantly reduced wind-generated noise, however, it had the disadvantage of retaining water from precipitation (rain or snow). Work is still required to find an optimum cover material with good wind-noise-suppression characteristics, but which will not retain water. This remains a potentially serious problem for an operational system.

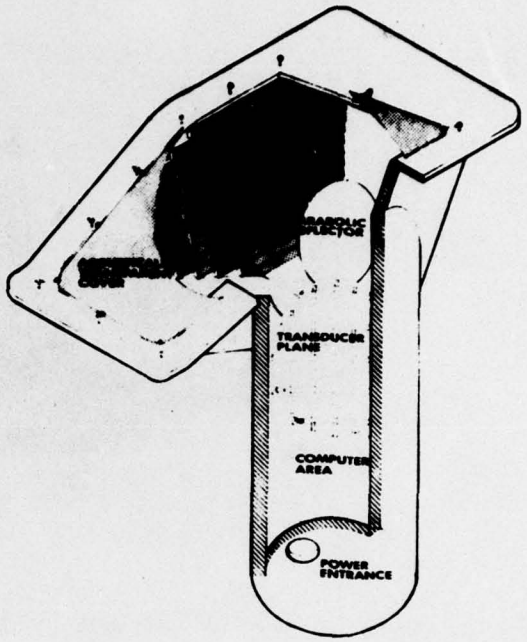

Figure 8. Isometric cutaway view of the Table Mountain receiver bunker.

The inside of the prototype bunker is shown in Figure 10. The off-axis parabolic antenna section appears in the upper left hand portion of the photograph and some of the seven transducers can be seen on the right. The recess containing the transducers is lined with sound absorbing foam and the honeycomb absorber appears on the left side of the picture.

3.2.2.2.3 Beam Patterns of Prototype Antenna

Beam patterns of the completed receiver antenna were measured by using the technique described by Willmarth et al. (1975) and are shown in the lower half of Figure 11. Each of the seven beam patterns, taken in a vertical plane containing the centerline of the bunker, are shown and can be compared with the corresponding theoretical patterns shown in the top half of Figure 11. The excellent agreement between the two sets of beam patterns is an indication of the success of the antenna design.

3.3 Ambient Noise Considerations

Because the noise from falling rain is known to be a problem, the Table Mountain prototype installation is equipped with a "tipping bucket" rain gauge. Rain rates measured by this device

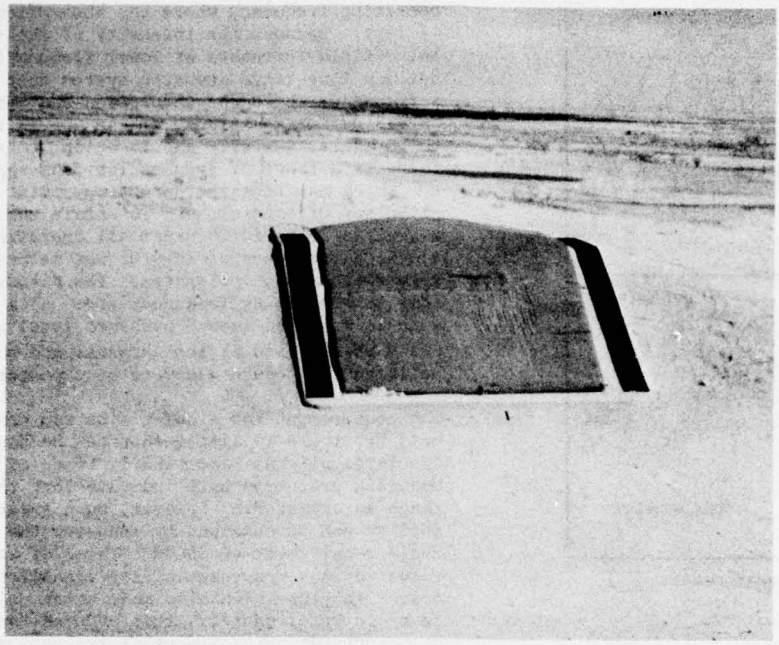

Figure 9. Table Mountain prototype receiver bunker shown with an acoustically transparent foam cover.

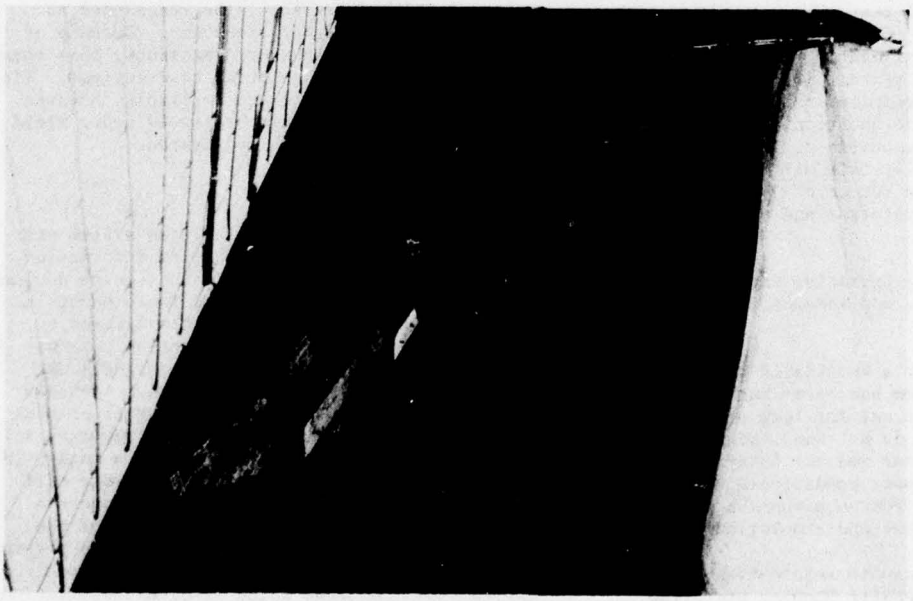

Figure 10. Interior view of Table Mountain receiver bunker.

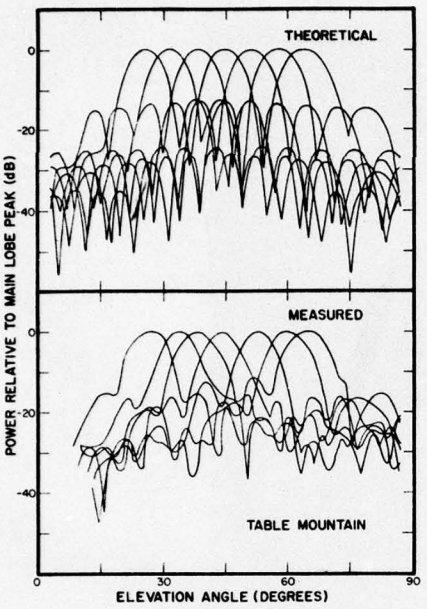

Figure 11. Theoretical and measured beam patterns of Table Mountain receiver antenna.

can be correlated conveniently with the measured signal-to-noise ratio of the system.

3.3.1 Solution to Minimize the Effects of Precipitation Noise

The first operational test unit will incorporate a small pulsed Doppler (EM) radar as a backup unit when rain noise significantly degrades the operation of the acoustic system. Because of the absence of liquid precipitation in Colorado during the winter months, the question of when to make the transition from acoustic to EM radar remains unanswered. Hopefully, this will be resolved during the spring and summer of 1976 by using data collected with the prototype and the first operational test systems.

3.3.2 Optimum Range, Operating Frequency, Ambient Noise, and Antenna Size Considerations

The optimum range for a vertically profiling windshear detection system has never been clearly established. This is not for lack of opinions, but because we still do not know enough about the structure of wind shear and the interaction of aircraft with wind-shear conditions. These answers can only come from an extensive and well-coordinated measurement and simulation program.

In the absence of adequate information on range requirements, the acoustic Doppler prototype system was designed to reach an altitude of 1 km. However, severe penalties must be paid for this altitude capability. At these ranges, atmospheric attenuation of sound becomes a significant factor and must be compensated for by using a rather low operating frequency where the absorption of sound is less. Because the intensity of the ambient noise field increases at lower frequencies, the optimum long-range acoustic system must operate at a frequency where the absorption and ambient noise curves define a minimum. These curves vary with temperature, humidity and location, consequently, there is a range of frequencies from about 1 to 4 kHz which may contain the optimum point under any given set of conditions. To obtain the maximum signal-to-noise ratio under all operating conditions, a frequency of 1250 Hz was selected for the 1 km range prototype system. The disadvantages of this low operating frequency are: a) a very quiet site is required (sound pressure level below 15 dB re 20 $\mu N/m^2$), and b) the antennas and bunkers must be large to produce adequate beam patterns.

The requirement for a quiet site can usually be met, but there is little that can be done about the large antenna size. Early tests of the Table Mountain prototype unit indicate that the 1 km range is achievable, however, much greater reliability can be obtained by reducing the total range requirement to 500 m. This, of course, resulted in a reduction of the transmitter-receiver spacing which also made attenuation less severe. Unfortunately, this reduced range requirement was not fixed until the operational test system development which proceeded in parallel with the Table Mountain prototype tests had gone beyond the point where the antenna and bunker sizes could be changed. Because of the uncertainties in range requirement, the operational test system was designed to operate at either 1250 or 1750 Hz. For future systems that have range requirements less than 500 m, the frequency should be increased to the range of 2 or 3 kHz and the antennas and bunkers should be redesigned to accommodate this higher frequency. Because of the reduced antenna and bunker dimensions, this change would result in a substantial cost savings. These changes appear feasible and desirable, however, the altered design should be tested under field conditions before it is implemented.

3.4 Software Requirements

The computer in the early Stapleton system was used mainly to process the Doppler information extracted from analog signal-conditioning devices. The role of the computer in the Table Mountain prototype system was significantly altered by giving it the system control function. Rather than just simply accepting analog signals at predetermined times, the computer now controls the pulse repetition rate and the receiver beam steering, and extracts the Doppler frequency shift from spectral information derived by a hardwired FFT unit. This change has made much more efficient use of the computer, and has produced a significant improvement in the quality of the Doppler information. In addition, it was possible to introduce a more sophisticated noise spectrum subtraction technique which involves subtraction of the averaged noise spectra from the noise-contaminated signal spectra.

3.4.1 Noise Suppression

The state-of-the-art in both Doppler extraction and acoustic noise suppression techniques has been advancing in parallel with the development of the prototype and operational test units. An adaptive inverse filtering process (Keeler and Griffiths, 1977) shows promise for replacing the FFT-derived spectra for determining the Doppler shift. In addition, more sophisticated noise suppression is possible by using similar adaptive methods in conjunction with different noise sampling techniques. These development efforts are proceeding and will be tested in the prototype unit. If these techniques improve the system performance, as it is expected, they can be introduced into the operational test unit by making software and minor hardware modifications.

3.5 Summary of Phase III Engineering Development

The engineering development work described above was essential to the design of the first operational test unit installed at Dulles Airport. This prototype development unit served as a test bed for the hardware and software that were developed for the Dulles system. Because the final design work for the operational test system was started literally during the same month as the Table Mountain installation became operational, this system has not operated in the traditional prototype mode. Design changes and field alterations of various system parameters were constantly being made and the equipment could not be operated in an unattended, unmodified test mode for extensive time periods. In addition, many of these changes altered the system performance, making it very difficult to collect the data base needed for judging the overall reliability of the system. This is perhaps one of the greatest penalties paid for the unorthodox, parallel prototype and first operational system development approach.

Following the installation of the Dulles system, the Table Mountain prototype reached the stage where it can be used more extensively for comparison measurements with standard wind sensors and other remote wind-measuring equipment. This continuing work will provide a valuable data base which can be combined with that from the Dulles system for assessing the overall reliability of acoustic Doppler techniques. A preliminary report on the first six months of operation of the Table Mountain system is contained in Appendix C.

The Table Mountain facility will also continue in its role as a test bed for system modifications. New concepts for improving the Dulles operation are being developed and tested at Table Mountain before they are introduced into the operational setting, thus reducing the down time of the operational system to a minimum.

4. A REVIEW OF WIND-SHEAR TYPES AND THEIR DETECTION

At the inception of this program it was believed that the generation of dangerous wind-shear conditions was associated with synoptic-scale features such as frontal surfaces, and possibly the interface formed by a strong nocturnal inversion. It was recognized that wind shear was also associated with the cold air outflow from a thunderstorm, the "gust front", but the danger from this phenomenon was not perceived to be as great. The history of wind-shear-related aircraft accidents that have occurred since the project started indicates that this assumption was incorrect. The majority of these accidents appear to be associated with thunderstorm-produced gust fronts.

A vertically pointing system, like the acoustic Doppler, that can measure a wind profile to heights of around 0.5 km at one location near an airport should detect the majority of synoptic-scale wind-shear events. If the horizontal homogeneity assumption is valid, this single vertical wind profile would provide the wind-shear detection and warning capability needed to prevent the occurrence of accidents such as the Boston Iberia Air Lines DC-10 crash in 1973.

However, these systems are not intended to detect the far more transient gust front, which can approach an airport from any direction and will produce a very localized mesoscale effect. The gust front will be detected only if it passes directly over the instrument location, a chance that cannot be taken for a reliable warning system.

Clearly, if the gust-front-generated wind shear is to be detected, a single vertically pointing wind measuring system is not adequate. Ultimately a sensing system which has a rather long range (up to 20 km) and which can scan the entire region around an airport, including the approach and departure paths will be required. Such systems are feasible, but are still a few years away from operational deployment.

The increasing incidence of gust-front-related accidents makes a solution to this problem important. A detailed analysis of the gust-front detection problem is presented by Bedard and Beran (1977). It is shown that gust fronts have three readily detectable features, all of which occur at or near the surface: a sharp change in wind speed and direction, a sharp rise in pressure and a drop in the surface temperature.

Meteorological instruments presently installed at all airports will indicate the presence of a gust front, but usually too late to provide any warning for aircraft. It has been suggested that by placing anemometers at the middle marker an extra margin of safety would be provided for incoming aircraft. While this may be partially true, such a scheme would still provide little advance warning to an approaching aircraft since the gust front would already be at the middle marker and would create a dangerous situation before any warning could be given. To increase the warning time, the sensors must be placed several miles from the airport and must completely surround it.

The choice of an optimum sensor for this purpose is still to be decided. Preliminary indications are that wind and pressure changes are equally good indicators of gust-front passage. If this is confirmed, then the question of which sensor to use can be answered by comparing the cost and complexity of the anemometer and the pressure jump

detector (see Bedard and Beran, 1977). Because the pressure jump detector in its present form is a passive device which is quiescent until triggered by the scalar pressure change, it appears to be simpler and much less expensive. In contrast, the anemometer must remain active continuously and sense both the speed and direction of the wind. The vector wind information is more difficult to transmit and process than the simple scalar pressure data.

Pressure trigger levels, which indicate the presence of only those gust fronts which are hazardous, still need to be determined, although a rather narrow range of values can be defined based on our present understanding of the gust front. Studies of aircraft response to various gust-front conditions are also needed before an optimum trigger level can be determined.

The detection of gust fronts using pressure jump sensors can provide a valuable addition to the vertically profiling system. It is important to recognize that they are capable of indicating only the arrival of potentially hazardous conditions produced by transient, thunderstorm-related phenomena. They may not detect synoptic-scale shear conditions, nor will they give a precise indication of an "all clear".

An optimum wind-shear detection system must combine the ability to measure the vertical profile of wind with a provision for sensing the passage of a gust front well before it reaches the airport's active approach and departure paths. Within the present limits of technology, this optimum capability can be achieved only with a combination of sensors such as that installed at Dulles airport. The cost-effectiveness of such an elaborate system is open to debate, however, for the time being it remains the only operational system which can provide an effective total wind-shear warning capability.

5. SECOND-GENERATION WIND-SHEAR DETECTION SYSTEM DEVELOPMENT

While work has been progressing toward the first-generation systems described above, technological developments have indicated that more advanced, second-generation detection concepts are feasible (Huffaker, et al., 1976). As described previously, a second-generation system is one which could replace the vertically profiling device and ground-based arrays with a single sensor designed to scan over the entire region around the airport and detect approaching gust fronts as well as wind shear along approach and departure paths. The main advantage of such a system would be its greater cost effectiveness when compared to first-generation devices. Lasers and EM radars are the two sensors that now appear to have the necessary capability of becoming effective second-generation systems.

5.1 Laser Systems

In the past, laser systems have been downgraded because of their relatively early stage of development. Questions concerning their ability to penetrate cloud or fog and the availability of aerosols for tracers have been partially answered only recently. Work with CW Doppler lasers has demonstrated that the availability of tracers is probably not a serious concern, especially when sophisticated processing techniques are used to improve the signal-to-noise ratio. The CW Doppler laser still has the drawback of having poor range resolution at distances exceeding 1 km. For this reason, its optimum operational mode is to measure a vertical wind profile using Velocity Azimuth Display (VAD) scanning, making it a viable first-generation alternate for the acoustic Doppler.

A more advanced sensor using a pulsed CO_2 laser does not suffer from the serious range resolution limitations inherent in the CW system. Studies conducted by NASA (Huffaker, private communication) indicate that the pulsed CO_2 lidar has good cloud and fog penetration ability and could possibly provide the all-weather capability needed in a second-generation system.

5.2 FM-CW Radar

Within the last year, improved processing methods have made it possible to detect clear-air echoes with microwave radar. This major technological breakthrough was accomplished with an FM-CW radar (Chadwick et al., 1976) but is also applicable to pulsed radars using sufficiently large antennas.

Prior to the above advances in radar technology, radar systems were considered unacceptable for shear detection, because of their need for artificial tracers. If ongoing research demonstrates that clear-air radar echoes and Doppler shifts can be detected with high reliability, then this system will become a prime candidate for the second-generation system.

A radar has several significant advantages over other types of sensors. For example, its ability to operate during inclement weather should be excellent, because of the added tracers in the form of hydrometeors. From a cost-effectiveness point of view, introduction of a new type of radar at airports would have less impact on the operations than a system based on one of the newer technologies such as lasers. Technicians already trained in radar maintenance would be available more readily, thus reducing the need for new manpower and training requirements. In addition, many of the spares now stocked for standard airport radars might also be useable for the new devices. While these factors should not be allowed to override the importance of first proving the radar's capability, they are important and could be the determining factor in the final selection of an optimum second-generation sensing system.

The important ability to scan the region around the airport to ranges of several km is characteristic of both the radar and some types of laser systems. A potential weakness of these systems is that they are able to measure only the radial component of the wind. Recent theoretical work (Lee, 1976) suggests the possibility of a new processing technique which could be used to measure both transverse components as well as the

radial component of the wind at any point within the range of the sensor. The technique has been suggested for use with a laser system, but it may be applicable to radars as well.

6. SUMMARY AND RECOMMENDATIONS

Based on the Table Mountain prototype development and subsequent testing, the basic design for the first-generation operational test unit has been fixed. This dual acoustic EM Doppler radar system augmented with an array of pressure sensors will be operating at Dulles International Airport. The acoustic portion of the system consists of a powerful vertically pointing transmitter which is surrounded on 120° radii by three receivers spaced 290 m from the transmitter. Any two of the three receivers are sufficient to produce a wind profile, thus providing a degree of redundancy. Each receiver antenna beam is steered to seven positions, and with the aid of satellite transmitters (located 50 m in front of each receiver) they can cover a height range from 30 to 510 m. The operating frequency for this unit is selectable between 1250 and 1750 Hz. Less ambient noise is expected at the higher frequency and with a total range requirement of only 500 m, atmospheric absorption should not be a serious problem. The effect of rain noise on an acoustic system has not been fully established, simply because the prototype has not been operated for a sufficient length of time to produce the needed data. The limited experience that has been gained indicates that acoustic devices will be rendered inoperable during heavy rain. To compensate for this loss of signal during rain, a small pulsed EM Doppler radar has been added to the vertically profiling portion of the Dulles system. It has been shown that winds can be measured with the radar when hydrometeors are present, (Lhermitte and Miller, 1970), but the dual-sensor concept itself is untested. This aspect of the Dulles system is only a conceptual test and should not be considered as an operational part of the system. Tests to date are very promising, therefore, the radar could be replaced by a permanent unit.

The final portion of the first-generation Dulles system will consist of a ground-based array of pressure sensors around the airport. These units will be triggered by the passage of gust fronts and will provide information on their position and speed. This portion of the system is also untried and will become part of the operational system only if the tests are successful.

The rather complex array of sensors which make up the total first-generation Dulles system has the potential of solving the wind-shear warning problem. Given the present state-of-the-art in detector technology, it is also the best that can be provided at this time. The total system is expensive and, when compared with potential second-generation sensors, it may not be the most cost-effective approach. For this reason, it is recommended that no additional acoustic systems be installed, at least not until the second-generation systems can be field tested.

By proceeding in this manner, the wind-shear detection problem will remain unsolved until the second-generation systems become operational. Recognizing that the majority of recent accidents have been caused by thunderstorm-related phenomena, a less-expensive partial interim solution is available. A degree of protection could be provided by equipping all major airports in regions exposed to high thunderstorm incidence with some form of the pressure jump detector array. The cost of such installations would be a fraction of the total Dulles system cost and could be implemented rapidly. These sensors would provide only a warning of dangerous gust-front conditions and would not be effective for giving information on shear magnitude nor for indicating an all-clear condition following the passage of the gust front. A statistically-determined delay time after a gust-front passage could be used to project an "all-clear". More extensive use of available forecasting techniques would also help to alleviate the problem of shears associated with synoptic-scale features (Sowa, 1974).

REFERENCES

Bedard, A. J., Jr., and D. W. Beran (1977). Detection of gust fronts using surface sensors, NOAA Tech. Memorandum, ERL WPL-20, 15 pp.

Beran, D. W. (1974), Remote sensing wind and wind shear system, FAA Report No. FAA-RD-74-3.

Chadwick, R. B., K. P. Moran, R. G. Strauch, G. E. Morrison, and W. C. Campbell (1976). A new radar for measuring winds, Bull. Amer. Meteorol. Soc., Vol. 57, No. 9, 1120-1125.

Huffaker, R. M., D. W. Beran, and C. G. Little (1976). Pulsed coherent lidar systems for airborne and satellite based wind field measurement, Preprint Volume, Seventh Conference on Aerospace and Aeronautical Meteorology and Symposium on Remote Sensing from Satellites, Nov. 16-19, Melbourne, Florida. Published by the AMS, Boston, Massachusetts.

Keeler, R. J., and L. J. Griffiths (1977). Acoustic Doppler extraction by adaptive linear-prediction filtering, J. Acoust. Soc. Am., Vol. 61, No. 5, 1218-1227.

Kurze, U., H. Erdmann, B. Schneider, and E. Steffen (1975). Zwischenbericht III über die Entwicklung und Erprobung einer Anlage für die indirekte sondierung der Atmosphäre mittels schallimpulsen, für das Bundesministerium der Verteidigung, Rü Fo 3a, Bonn BF-R-62.076-3, November 1975.

Lee, R. W. (1976). Transverse velocity measurement with Doppler radars, Lassen Research Report No. LR-7601, Prepared under NOAA Contract No. 01-6-022-15793, 42 pp.

Lhermitte, R. M., and L. J. Miller (1970). Doppler radar methodology for the observation of convective storms, Preprint Volume, 14th Radar Meteor. Conf., pp. 133-138.

Nagarkar, B. N., and R. D. Finch (1975). Acoustic model study of a Doppler wind monitor receiver bunker, NOAA Reports No. 01-5-022-2382 and No. 01-6-022-12172, 61 pp.

Sowa, D. F. (1974). Low-level wind shear, DC Flight Approach, No. 20, Douglas Aircraft Company, pp. 10-17.

Willmarth, B. C., E. H. Brown, J. T. Priestley, and D. W. Beran (1975). Beam pattern measurements for large acoustic antennas, Preprint Volume, 16th Radar Meteorol. Conf., Houston, Texas, pp. 278-281.

Wirt, L. S. (1973). The design of sound absorptive materials to meet special requirements, Lockheed Rept., presented at 86th meeting, Acoust. Soc. of Amer., Los Angeles, California, 80 pp.

APPENDIX A

ACOUSTIC COUPLER DESIGN

J. T. Priestley

This Appendix briefly describes the measurements of acoustical impedance which were necessary as a prerequisite to the design of the weather-proof acoustic couplers to be used in the transmitter array.

Consider a horn driver connected to a cylindrical coupler as shown in Figure A1. It is possible to design the coupler — determine its length and diameter — in such a way that the specific acoustic impedance (SAI) in the connecting tube is just ρc (ρ is the density of air and c is the speed of sound) and thereby couple to the atmosphere at near maximum efficiency. Although this is simply stated, the actual procedure involves using a computer to iteratively solve a set of nonlinear equations. As an input to the computer program one must provide either a mathematical function or a look-up table giving the complex SAI of an open-ended tube versus the parameter ka (k is the wave-number and a is the radius of the coupler tube).

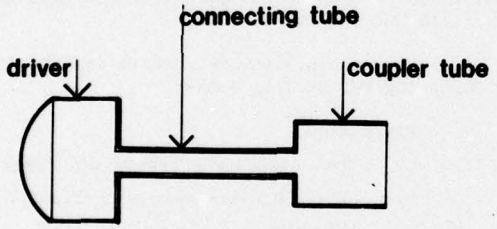

Figure A1. End-fire coupler.

The SAI has been computed[1] for the configuration given in Figure A1. Because of the requirement for weather-proofing, we attempted to design a coupler of the configuration shown in Figure A2.

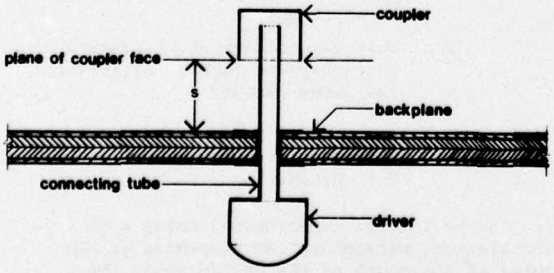

Figure A2. Mushroom coupler.

[1] Levine and Schwinger, Phys. Rev., 73:381 (1948).

This coupler can be designed with the same computer program used to design the end-fire coupler of Figure A1 if we substitute the appropriate mathematical expression or look-up table for the complex impedance looking out of the coupler at the plane of its face. Unfortunately, no one has computed this impedance and it is much more complicated than that for the Figure A1 case. Instead of being a function of only the one parameter ka it is a function of three parameters; ka, kb, and ks where b is the outside radius of the connecting tube and s is the separation between the coupler face and the backplane.

Because measuring the complex SAI as a function of three independent parameters would have been quite an intractable task, some scheme had to be devised to either eliminate or reduce the range of one of the parameters. This was accomplished by making a series of free-field measurements in which the on-axis farfield sound pressure was measured as a function of s for several different diameter couplers. Since we were only interested in the maximum pressure as a function of s, it was possible to derive an empirical relationship between ks and ka. (The relationship is $ks = \pi + .27\ ka$).

With the number of independent parameters reduced to two — ka and kb — the experimental apparatus diagrammed in Figure A3 was constructed. The

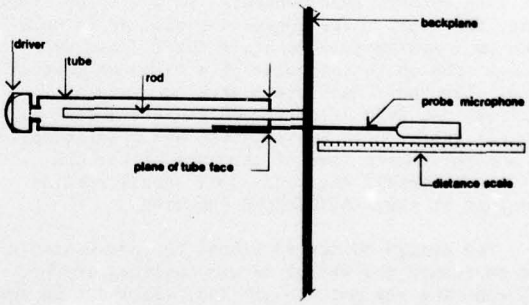

Figure A3. Measurement of complex impedance

actual experiment consisted of about ten series; each series consisting of about a dozen runs. To make the experiment more amenable to the physical constraints, the measurements were taken in terms of the parameters b/a and ka. The runs within a given series — fixed b/a — were made as a function of ka by changing the frequency and hence k. Each new series was accomplished by changing to a new rod of different radius b thus changing the parameter b/a.

The measurement procedure for a given run was to slide the microphone along a rail thereby inserting the microphone probe into the standing wave tube. The position of the microphone was carefully adjusted to find a maximum on the oscilloscope and then both that voltage and position were recorded. This process was then repeated for the next extrema until the voltage and position of typically the first six extrema were recorded. To set up for the next run; (1) the putty and tape around the rod guy wires were removed; (2) the spacing s between backplane and tube end was changed to the next setting; (3) the putty and tape were replaced; (4) the air temperature was measured and the frequency corresponding to the next ka was computed; and (5) the oscillator and the detector filter were set to the new frequency. In order to start a new series of runs — change b/a — the rod had to be removed and replaced with one of a different radius.

This procedure made it possible to design an acoustic coupler simply by specifying the diameter of the connecting tube and the signal frequency. Without this impedance information each coupler design would have involved a trial and error procedure taking up to six weeks per coupler type.

APPENDIX B

INTERIM MEASUREMENTS ON FAA PROTOTYPE ACOUSTIC TRANSMITTER

J. T. Priestley

1. INTRODUCTION

The type of acoustic transmitter under consideration is composed of a 2 meter diameter conical horn reflector (CHR) antenna, and a manifold with a number of electroacoustic drivers. The CHR antenna consists of a cone with horizontal axis and a large parabolic reflecting surface at the large end. Spherical wave fronts traveling along the horizontal cone are reflected upward at the parabolic surface, emerging as a narrow beam of plane waves.

The "old" manifold system consists of twelve JBL 2482 drivers each connected to a 2" I.D. steel tube, the steel tubes converging such as to maintain an approximately constant total cross-sectional area up to the point of attachment to the cone. The "new" manifold system consists of thirteen JBL 2470 drivers each connected to a conical tube. Each conical tube has a solid angle of one-thirteenth that of the cone of the CHR antenna therefore the total solid angle remains constant at the manifold/CHR junction.

The design objective behind the new manifold was to reduce the effect of air nonlinearity by, (1) reducing the path length and, (2) reducing the acoustic pressure as soon as possible with the conical tubes whose cross-section began to increase immediately at the driver mouths. This objective was at least partially compromised by the need for going to the smaller JBL 2470 drivers whose mouth diameter was only half that of the large drivers. The smaller drivers were needed because of the additional requirement of a higher operating frequency (1750 Hz as well as 1250 Hz) and the concurrent problem of geometrically packing the drivers as it related to higher-order-mode effects within the manifold at the higher frequency.

The transmitter with the old manifold was placed in service at Table Mountain in November 1975. It was immediately apparent that the transmitted tone burst was significantly distorted. It was concluded that the distortion was probably due to a driver malfunction and not air nonlinearity. The signal amplitude was reduced until the distortion was judged subjectively less objectionable, and the system was run in this mode until late March 1976.

In late March plans were made to investigate the following two problem areas:

1. Distortion
   a. What caused the jagged waveform?
   b. Is air nonlinearity a problem?
   c. Does the new manifold improve air nonlinearity?
2. Efficiency and power output.
   a. What are the antenna beam patterns at 1250 Hz and 1750 Hz?
   b. What is the efficiency of the transmitter with each manifold and at each of the above frequencies?
   c. What acoustic power outputs can be expected?
   d. What can be done short-range and long-range to improve efficiency and power output?

2. EXPERIMENTAL FINDINGS

2.1 Distortion

In the initial experimental setup a GR Type 1962 electret microphone was suspended at the center of the mouth of the CHR antenna, the microphone element being about eight inches below the plane of the mouth (Figure B1). Table B1 shows the results of measurements taken in this manner using the old manifold at a frequency of 1250 Hz. It should be noted that before any changes were

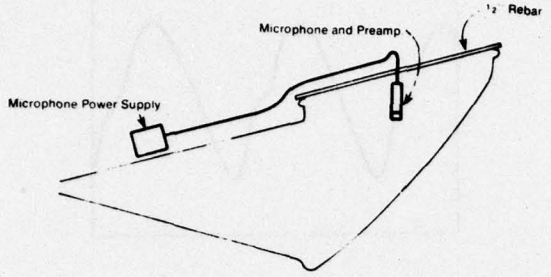

Figure B1. Microphone position for measurements in Table B1.

Table B1. Observations at 1250 Hz using old manifold.

Nature of signal	Dial setting of old sig. generator	Voltage at drivers (rms volts)		Microphone voltage		Microphone waveform
		measured with Dana DVM	deduced from dial setting	rms from Dana DVM	peak-to-peak from scope	
continuous	50	7.05		.39 to .47		clean (sinusoidal)
"	100	13.88		.76 to .85		some second harmonic visible
pulsed	100		13.88		2.5 to 2.6	" " " "
"	200		27.76		4.8 to 5.2	see Figure B3
"	210		29.15		5.4	similar to above
"	220	Power amplifiers just clipping				small rough spots
"	283	Power amplifiers severely clipping				rough and jagged

made the amplitude dial on the signal generator was set at 200.

From the information tabulated in Table 1 we can make the following conclusions:

1) The jagged waveform was due to clipping in the power amplifier.

2) The highest voltage the amplifiers can put out without clipping is approximately 29 volts rms.

3) With about 13 volts delivered to the drivers, second harmonic distortion just becomes evident.

4) At 28 to 29 volts into the drivers the waveform at the microphone (Figure B3) tends toward the classical sawtooth wave shape except for the small bump on the steep part of the waveform. We therefore tentatively conclude that the distortion is due to air nonlinearity.

In an attempt to remove the doubt from conclusion #4, a one-ohm resistor was successively put in series with several of the drivers and the current waveforms were observed. Because the waveforms had no visible distortion, we conclude that the motion of the diaphragm is sinusoidal and the distortion must have occurred after the drivers.

At this point the small bump in the pressure waveform remained an unresolved question, because it is definitely not a characteristic of air nonlinearity. From Figure B1 we can see that it is possible for sound to arrive at the microphone along two paths of different lengths, a direct path and a reflected path. Therefore a likely explanation is that the extra bump in the waveform is caused by the addition of two complex waves. To confirm this hypothesis the microphone was placed against the reflector (Figure B2) thereby virtually eliminating the difference in path lengths between the direct and reflected paths. The extra bump was indeed eliminated

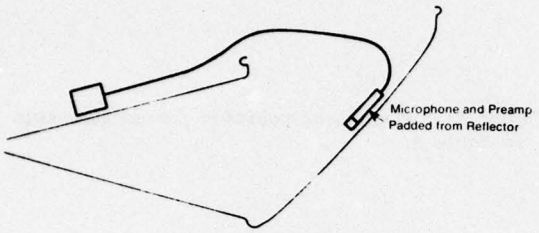

Figure B2. Microphone positioned at center of reflector.

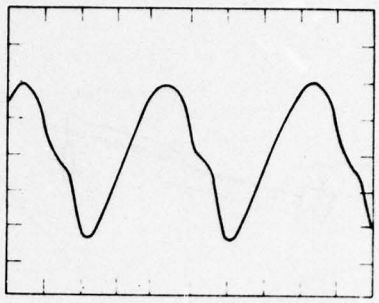

Figure B3. Microphone output with microphone positioned as shown in Figure B1. (one div = 848 dynes/cm^2.)(Negative pressure is up.)

(Figure B4a) therefore we conclude that up to the point of amplifier clipping all of the distortion is caused by air nonlinearity.

Figures B4a through B4d show the waveforms with the microphone in the center of the reflector for both the old and new manifolds at 1250 Hz and 1750 Hz. In all cases the input voltage to the drivers was below the clipping level of the amplifiers. The 1250 Hz waveforms both for old and new manifolds exhibit a not-fully-developed sawtooth wave shape characteristic of air nonlinearity, although the one for the old manifold also exhibits an asymmetry from top to bottom. The 1750 Hz waveforms both exhibit the beginning stages of the sawtooth waveform along with a small amount of top-to-bottom asymmetry. The cause of this top-to-bottom asymmetry is presently not understood. Microphone distortion is one possibility; the SPL of the 1250 Hz signals is about 142 dB and the upper end of the dynamic range of the GR microphone is only 145 dB. This explanation, however, presents the following problems:

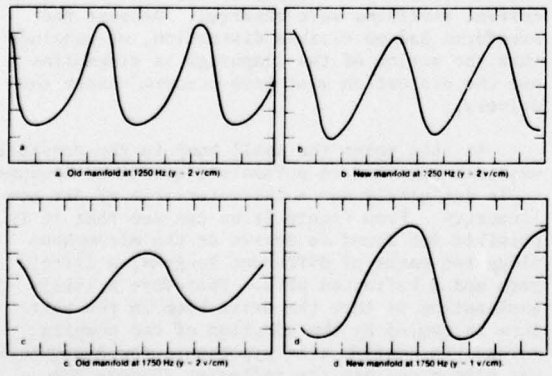

Figure B4. Output of microphone with microphone placed at center of reflecting surface. (One volt corresponds to 848 dynes/cm^2.) (Negative pressure is up.)

(1) Both of the 1250 Hz waveforms are about the same amplitude, but only one of them exhibits this particular asymmetrical distortion.

(2) While both of the 1750 Hz waveforms are asymmetrical their asymmetry is opposite in sense.

In spite of a foam pad between the microphone and the reflector, another possible explanation is that the microphone might have picked up a contaminating signal through structure-borne vibration. The phase of this contaminating signal would, of course, not be expected to be the same between the old and new manifolds, and this could explain the asymmetry in the waveforms.

2.2 Efficiency and Power Output

In order to measure the acoustical output power, beam pattern measurements (Figures B5 through B8) were made using a balloon-supported microphone which was swung in an arc over the transmitter. The power in the beam was calculated by using the curves to numerically integrate over a cone of approximately 10 degrees half-angle.

Beam patterns at 1250 Hz and 1750 Hz were taken with the old manifold. For each beam pattern the sound pressure was measured at the center of the reflector (Figure B2). In this way a relationship (at each frequency) could be established between the sound pressure at this point and the acoustical power in the beam. With the new manifold the sound pressure was again measured at the center of the reflector and — under the assumption that the manifold did not affect the beam shape — the beam power was calculated. All of the measurements were made at an amplitude at which no distortion was noticeable.

The voltage, current, and phase angle at the drivers were measured and the resulting electrical input power was calculated. From these measurements the electrical to acoustic beam power efficiencies were calculated and are presented in

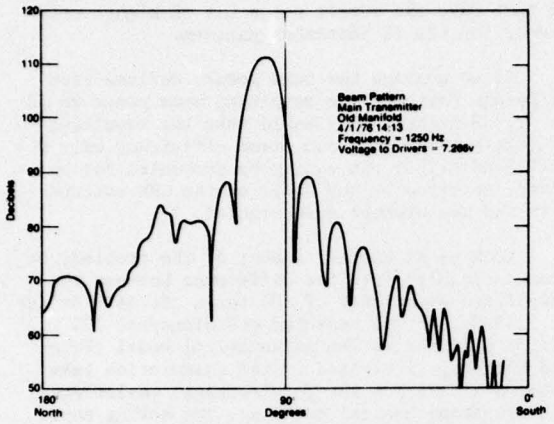

Figure B5. CHR antenna beam pattern at 1250 Hz (North to south)

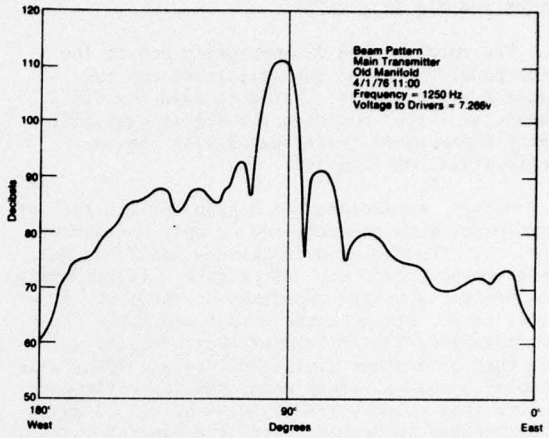

Figure B6. CHR antenna beam pattern at 1250 Hz (West to east.)

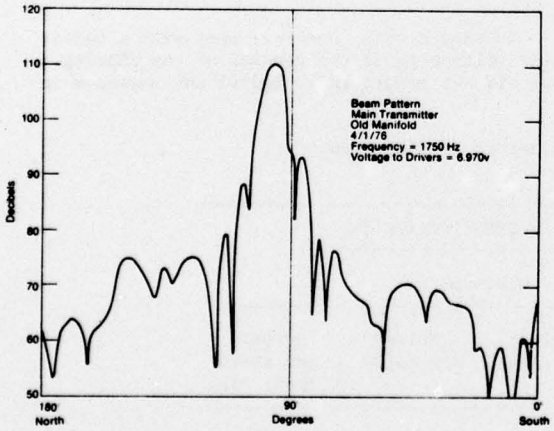

Figure B7. CHR antenna beam pattern at 1750 Hz (North to south.)

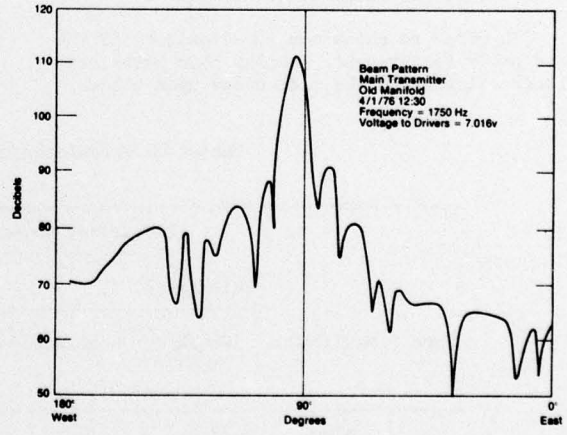

Figure B8. CHR antenna beam pattern at 1750 Hz (West to east.)

column 4 of Table B2. Column 3 contains the calculated efficiencies from a mathematical model (Finch and Higgins, 1976).

The results were disappointing due to the discrepancies between the calculated and the measured efficiencies. Not only were the discrepancies large, but also the significant efficiency improvement, anticipated with the new manifold was not obtained.

Efforts to isolate the reason for the lack of improvement were concentrated on only one driver type, the JBL 2470 used in the new manifold, and one frequency, 1250 Hz. After carefully tailoring the specific acoustic impedance at the mouth of a driver to ρc, its acoustic output and power input were measured. The efficiency thus obtained was 16%; that of another similar driver was 18% (Table 2, cols. 5 and 6). This means that an efficiency decline from roughly 17% to 10.2% or 2.2 dB must be attributed to problems with the manifold-horn system and/or measurement errors. Similarly, the efficiency difference of 60% (theoretical) down to 17% (measured) must be accounted for in terms of problems with the model and possibly measurement inaccuracies.

Of the 2.2 dB difference observed between the individual drivers and the beam power measurement, 0.8 dB can be attributed to energy diffracted into sidelobes (Born and Wolf, 1964). Another 0.6 dB can be attributed to atmospheric absorption (Beranek, 1949). An additional 0.1 to 0.5 dB can probably be attributed to differences in acoustic loading. We have so far accounted for all but 0.3 to 0.7 dB of the original difference.

In order to check the repeatability of the beam power measurement, another beam power efficiency calculation was made based upon a beam pattern taken on 10 September 1975. After taking into account the different atmospheric absorption of that day, the result was a 0.4 dB higher efficiency for the 10 September pattern.

If we average the beam powers derived from different patterns the resulting beam power would be 0.2 dB higher. This would make the remaining deficit between the beam power efficiency only 0.1 to 0.5 dB. This can easily be accounted for by energy absorbed by the walls of the CHR antenna horn and measurement inaccuracies.

Looking at another aspect of the problem, we need to inquire into the difference between the calculated efficiency of 60% for a JBL 2470 driver at 1250 Hz and its measured efficiency of 17%, a 5.5 dB difference. The mathematical model (Finch and Higgins, 1976) used in the calculation takes into consideration the dc electrical resistance, the electromechanical coupling, the moving mass, the suspension stiffness, the suspension dissipation, and the radiation loading. The model does not consider the impedance transformation that takes place in the conical portion of the throat (it assumes a cylinder), the loading on the back side of the diaphragm, and the dissipation due to air viscosity.

On the assumption that one of the more significant deficiencies of the model is that it does not consider air viscosity losses, about two-thirds of the phasing plug was removed from one of the drivers. The results of measurements on this driver (Table 2) showed that the efficiency increased from 18.0% to 25.9%, an improvement of 1.4 dB.

We should note, however, that with a particular voltage input the removal of the phasing plug did not result in a significant increase in

Table B2. Calculated and measured efficiencies.

		Electrical to Acoustic Efficiencies (%)				
		Calculated	Measured			
Freq.	Manifold	Finch's model	beam power	driver ser #5613	driver ser #6199	driver ser #6199 without plug
1250 Hz	old	29.3	11.6			
	new	60.0	10.2	16.0	18.0	25.9
1750 Hz	old	18.5	4.6			
	new	43.3	6.3			

output power; rather it resulted in an increase in electrical impedance (from 21.1 to 29.1 ohms) with a consequent decrease in input power. Therefore if the input voltage is limited the removal of the phasing plug may not be worthwhile.

3. CONCLUSIONS

Due to the limited amount of time available for this project some of the questions that were originally posed cannot be answered definitively. However, we can answer some and make intelligent guesses for others.

3.1 Distortion

On the problem of distortion the following questions were posed:

(a) What was causing the jagged waveform?

(b) Is air nonlinearity a problem?

(c) Does the new manifold improve air nonlinearity?

To these we can answer:

(a) The jagged waveform was caused by amplifier clipping.

(b) Air nonlinearity is definitely a problem. (See Figures B4a - B4d).

(c) The new manifold provides some improvement over the old one. (Compare Figure B4a with Figure B4b). This conclusion is tentative because of possible problems with microphone nonlinearity and vibration pick-up.

3.2 Efficiency and Power Output

Regarding the efficiency and power output problems the questions were:

(a) What are the beam patterns at 1250 Hz and 1750 Hz?

(b) What is the efficiency of the transmitter with each manifold and at each of the above frequencies?

(c) What beam power outputs can be expected?

(d) What can be done short-range and long-range to improve efficiency and power output?

The answers to these questions are as follows:

(a) The beam patterns are given in Figures B5 through B8. Note that at both frequencies the center of the beam leans about 8 degrees toward the north and 4 degrees toward the west. Some of this is caused by the fact that the antenna is leaning 3 or 4 degrees toward the north. The remaining 4 degrees toward the north and the 4 degrees toward the west are due to errors in the measurement process.

(b) The beam power efficiencies of the transmitter with the old manifold are 11.6% and 4.6% at 1250 Hz and 1750 Hz, respectively. The efficiencies with the new manifold are 10.2% and 6.3%, respectively. Note that the figures for the new manifold were not deduced from their own beam patterns, but rather from reference to the old manifold beam patterns through the transfer measurements of the sound pressure at the center of the reflector. Because there is some question as to a possible small contamination of this transfer measurement by the vibration pickup of the microphone, the efficiency figures for the new manifold should be considered less accurate.

(c) On the basis of the above-measured efficiencies, impedances, and the approximate amplifier clipping limits, the maximum acousic beam powers would be as follows: for the old manifold 77 and 35.5 watts for 1250 and 1750 Hz, respectively, and for the new manifold 57 and 35 watts, respectively. When taking into consideration the distortion at these levels (See Figures B4a-B4d) more realistic estimates would probably be 60 to 65 watts and 32 to 34 watts for the old manifold at 1250 and 1750 Hz, respectively and 50 to 55 watts and 32 to 34 watts for the new manifold.

(d) An immediate increase in output power could be realized by increasing the electrical input power. The transmitter would then be limited primarily by air nonlinearity and in some cases the maximum power input to the drivers. These limitations would probably be about the same for both manifolds; in the general range of 60 to 70 watts at 1250 Hz and 45 to 55 watts at 1750 Hz. The longer-range improvements fall into two categories: (1) those concerned with reducing the effects of air nonlinearity; and (2) those concerned with obtaining more power out of the drivers. There are two approaches for the first category: predistorting the electrical input to partially compensate for the air nonlinearity, and distributing the source over a larger area (i.e. a larger horn or a number of horns).

There are many possible improvements for increasing the power output of the drivers, but all rely upon a better understanding of the driver and a better mathematical model.

4. RECOMMENDATIONS

The recommendations are of two classes, those that can and should be implemented immediately for the Dulles installation, and those that require more study and can be used in future systems and/or for retrofitting the Dulles system.

4.1 Immediate

A. Increase the electrical input power. The amplifiers reach their clipping point substantially before the drivers reach their maximum rated input power. Presently three amplifier channels are used, each channel driving four drivers in parallel. The use of six amplifier channels with each channel driving two drivers through a step-up transformer is recommended. In particular, each channel of a Crown DC-300A should be connected to the 4 ohm tap of an Altec 15067 autotransformer and the 8 ohm transformer tap should feed a pair of parallel-connected drivers (Figure B9).

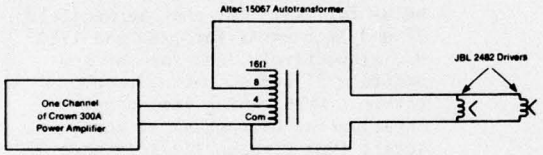

Figure B9. Recommended amplifier hook-up for each of six amplifier channels.

B. Send the old manifold to Dulles. Because the performance differences between the two manifolds are slight and since the new manifold is easier to model mathematically, the old manifold should be sent to Dulles and the new one should be retained for further study.

4.2 Future

The effects of air nonlinearity need to be investigated more thoroughly. Predistortion of the electrical waveform to compensate for nonlinearities could ameliorate the present situation. The interesting possibility of utilizing the second harmonic of the distorted wave for atmospheric probing should also be studied.

Improvements in the mathematical model of the drivers and manifold/horn assembly should suggest ways for increasing the overall electrical/acoustical efficiency.

5. ACKNOWLEDGMENTS

I am very grateful to M. Spowart and F. Mottola, for making the beam pattern measurements, and to H. Zimmerman, of Ball Brothers Corp., for his assistance throughout the series of Table Mountain measurements.

6. REFERENCES

Beranek, L. L. (1949). Acoustic Measurements, John Wiley and Sons, Inc., New York, 914 pp.

Born, M., and E. Wolf (1964). Principles of Optics, The Macmillan Company, New York, 808 pp.

Finch, R. D., and P. W. Higgins (1976). Optimizing the monotone performance of electrodynamic drivers using tubular couplers, J. Acoust. Soc. Am., Vol. 60, No. 4, 937-943.

Monin, A. S. (1962). Characteristics of the scattering of sound in a turbulent atmosphere, Sov. Phys. Acoustics, Vol. 7, No. 4, 370-373.

Simmons, W. R., J. W. Wescott, and F. F. Hall, Jr. (1971). Acoustic sounding as related to air pollution in urban environments, NOAA Technical Report ERL 216-WPL 17, 77 pp.

APPENDIX C

PROTOTYPE ACOUSTIC DOPPLER PERFORMANCE AT TABLE MOUNTAIN

F. Pratte

INTRODUCTION

In order to learn as much as possible about the wind measuring capabilities and meteorological limitations of the WPL acoustic Doppler system, selective analyses of regularly archived data from the prototype Table Mountain system and a comparison test with other wind sensors were performed. A discussion of some of the experimental problems and a summary of results follows.

The Table Mountain system has been collecting data in an unattended mode since early May 1976, whenever the system has been healthy and design changes were not being implemented. For this system, time-averaged wind data are recorded on digital magnetic tape including such items as signal and noise spectra, derived wind profiles, reliability figures, and surface meteorological parameters (wind, temperature, relative humidity and rain rate). In addition to the normal unattended operations, a special test period was arranged during the second half of June during which comparisons were attempted with another remote wind sensor, the FM-CW Doppler radar. A boundary layer profiler (BLP) tethered balloon, a monostatic acoustic echo sounder, and a 150 m instrumented tower were also in operation during the tests.

The goal of the field program is to elucidate information about the Table Mountain system in four categories: system reliability, meteorological operational limits, wind measurement accuracy and availability of acoustic scatterers, all under a wide range of conditions. The information obtained from this program facilitates design improvements of the experimental system. Complications involving ongoing system changes, coordination of various groups, and the meteorological limitations of the comparison sensors, have made the analysis of the data somewhat difficult. However, results of the data post-analysis suggest that the acoustic Doppler wind sensor is accurate to design criteria as measuring conditions permit and that it maintains reliability during adverse weather better than previously expected. In this report, an effort has been made to present statements and general observations about the system rather than firm conclusions. This tactic is warranted because of the nature of the measuring problem and the relatively small size of useable data sets containing the significant events.

COMPARISON TESTS

On June 24 and 25, 1976, data from several closely spaced sensors were gathered at Table Mountain. Besides the acoustic Doppler, an FM-CW Doppler radar, a tethered balloon (BLP), a monostatic acoustic sounder, and ground-based meteorological instruments were operating. Figure C1 illustrates the sensor layout. The test setup was located near the eastern edge of the mesa which is Table Mountain, and the site lies about 15 km north of Boulder and 5 km east of the first range of mountains. A 150 m instrumented tower was also in operation during the tests about 2 km WNW of the test site on the western edge of the mesa.

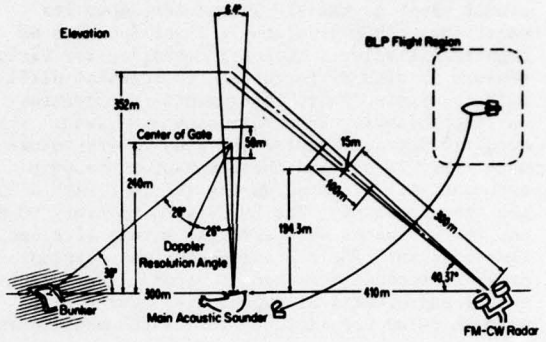

Figure C1. Schematic diagram of remote sensor wind comparison test setup at Table Mountain during June 76. Acoustic sounder and FM-CW radar were positioned along an east-west road. BLP was tethered near main acoustic sounder and flies downwind.

Long-term wind comparisons between the acoustic and FM-CW radar systems were the primary goal of the intercomparison tests. The BLP balloon was expected to provide "ground truth" wind measurements, and the monostatic sounder to give qualitative information about boundary layer stability.

Wind conditions on the two test days were nearly ideal. June 24 was marked by a moderate surface pressure gradient giving reasonably steady easterly winds in the boundary layer. Cool, dry, very clear conditions prevailed with relative humidities near 30%. June 25, on the other hand, was characterized by a weak pressure gradient; but downslope flow yielded occasionally strong westerly winds at the surface and very low humidities. Monostatic sounder records indicated weak thermal plume activity during the daytime on June 24 and well mixed conditions on June 25.

The acoustic Doppler and FM-CW radar were located along an east-west road about 400 meters apart. Both systems measured only the east-west wind component. The comparable sensed volumes were separated by about 200 meters at an altitude of about 200 meters.

The estimates of a measured quantity, in this case the speed of turbulent scatterers, from remote sensors are necessarily averaged both in time and space. Spatial averaging is related to the sensed volume size; the sizes of volumes for different

remote sensors are in general quite different. The acoustic Doppler volume is about 2.5×10^4 m^3, and the FM-CW volume is about 1.2×10^4 m^3. The orientation of the volumes will affect the degree of spatial averaging in any given wind field not aligned with the volumes. Naturally, an in-situ sensor, such as the BLP anenometer, does its measuring within a volume at least 5 orders of magnitude smaller. Temporal averaging for various sensors is also different and is somewhat difficult to assess due to instrumental differences, but the following information can be given. The acoustic Doppler sampled the wind in its volume once every 15 sec and these measurements were exponentially averaged during the test with a 30 sec time constant. The FM-CW samples every 50 ms and its estimates were averaged with a 12.8 sec time constant. The BLP anenometer was sampled every 15 seconds for about 1 second. Both mechanical and electrical exponential averaging of unknown value are included in the BLP measurement.

Remarks should be made about the influence of separation distance of sensors on the cross correlation of two wind measurements.

Correlation of measured winds at low frequencies is normally good, however it decreases rapidly as the scale of the measured phenomena approaches the separation distance. Using Taylor's hypothesis ("frozen turbulence") to convert time scales into space scales, the dropoff commences rapidly as the wavelength of the phenomena becomes smaller than 2π times the separation distance. Using this information, the minimum time scale (T), or maximum frequency, at which significant correlations will be found can be estimated from the separation distance (d) and mean wind speed ($\bar{u}$): $T = 2\pi d/\bar{u}$. For the comparison test, using a typical mean wind speed of 5 m s^{-1} and separation distances of 200 to 300 meters, $T \approx 4$ to 6 minutes. Good correlations may be found, but should not be expected for time scales smaller than these.

The BLP tethered balloon presented unique problems due to the instability of the measuring platform. The BLP consists of a helium-filled, dirigible-shaped plastic bag, tethered by a light dacron cable. The instrument package, suspended directly from the balloon, measures wind speed with a cup anemometer and wind direction by a compass-controlled potentiometer. Maximum flighttime is limited by available batteries to less than 3 hours. Under typical conditions a balance between free lift, aerodynamic lift, and wind drag on the tether line, all varying, determines the maximum useable altitude and the stability.

During good flight conditions at Table Mountain the sensor package can be expected to fluctuate ± 50 m in altitude and ± 25° in azimuth with occasional excursions of greater magnitude. This behavior puts some difficulty in the way of achieving a good wind comparison with other devices.

Certain additional experimental problems limited the wind comparisons between the acoustic and FM-CW radar systems. Some of the difficulties can be categorized under the heading of data management. These were resolved by employing a considerable amount of data processing. However, two related problems developed due to the layout of the sensors and the meteorological conditions. The low relative humidities both days precluded strong signal returns for the FM-CW radar which depends primarily on moisture inhomogeneities. Furthermore, a short metal tower located just east of the acoustic transmitter proved to be within the beam of the radar and required a substantial reduction in receiver gain to avoid overload. This tower could not be moved. The necessary reduction in gain frequently prevented accurate measurement of winds due to the low signal-to-noise ratio. Comparisons between remote sensors should include the specification that all sensors measure the same volume in space. It was not possible to achieve this requirement either, because of the radar receiver overloading from the metal tower. Additional comparison tests at the same location would not have been worthwhile because of the susceptibility of the radar to ground clutter.

RESULTS

Comparison results herein presented consist primarily of time series of wind data from sensors spaced several hundred meters or more apart in the horizontal and up to a hundred meters or so in the vertical. The differences in measured wind by each sensor is a result of several factors listed below:

1. The separation distance as well as the variation in separation distance in three dimensions. The correlation of wind fluctuations drops off as the scale of the phenomena (eddies, gusts, etc) approach the separation distance.

2. The remote sensors actually measure different, off-horizontal, components of the speed of the scatterers. The acoustic Doppler and FM-CW radar measured about 70° and 40°, respectively, off horizontal in this experiment. The wind values presented in the following figures are horizontal wind values computed from the diagonal components of scatterer speeds by simple geometry, under the assumption of zero vertical velocity. Though this assumption is rarely met in nature, over averaging times of the order of 10 minutes or so near-zero mean vertical velocity is probably attained for most times and places. Based on careful post analysis of data for consistency and continuity, it appears that false wind-shear indication at high gates due to vertical velocity fluctuations may be prevented by averaging for at least 6 minutes.

3. Differences in size and orientation of sensed volumes and different degrees of instrument inertia.

Despite these constraints, quite reasonable comparisons were obtained between the sensors for periods during which simultaneous data existed. The cases illustrated here show both east and west winds, in one instance above 10 m s^{-1}, at a "fixed" height. (See Figures C2 and C3). Wind correlations between sensors at the test site were

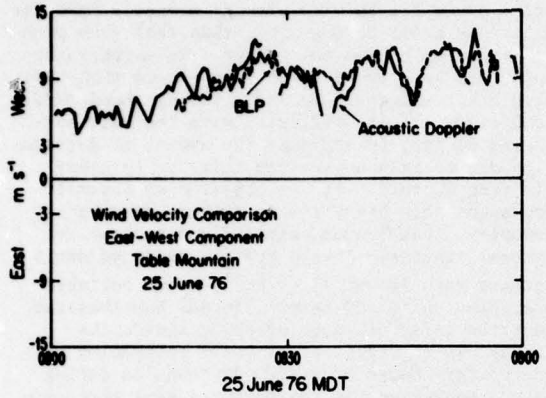

Figure C2. Comparison of westerly horizontal winds between BLP and acoustic Doppler. Acoustic Doppler winds were averaged with a two-minute time constant and lagged by the mean wind speed to improve correlation. Altitude was about 150 m AGL.

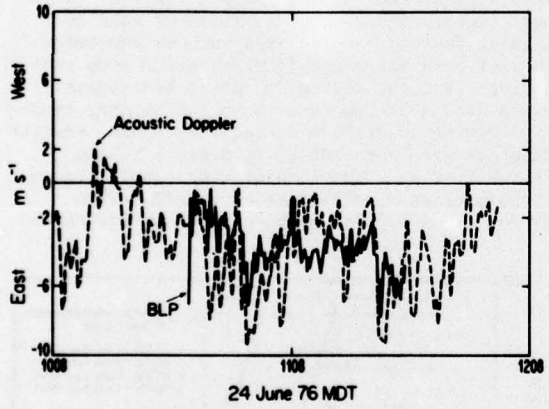

Figure C3. Comparison of easterly winds between BLP and acoustic Doppler. Acoustic Doppler winds were averaged with a two-minute time constant and lagged by the mean wind speed to improve correlation. Altitude was about 210 m AGL.

consistently good for scales larger than the separation distance. At the Table Mountain field site, there is a substantial difference in character between easterly and westerly surface winds. Easterlies generally occur under a low-level inversion, are governed by the surface pressure gradient, and demonstrate considerably more spatial and temporal persistence than westerlies. The downslope origin of westerly winds causes them to be quite unsteady due to the transport of high-momentum air to the surface through rugged terrain. With westerlies it is not unusual for large spatial speed gradients to exist under fair weather conditions, at times exceeding 0.02 s^{-1}. The best correlating time series with the instrumented tower 2 km distant to the northwest (shown in Figure C4) was found with easterly winds. As expected, under westerly downslope wind conditions less correlation was found. At distances of this magnitude in mountainous terrain one should not in general expect to find good correlations for time scales less than an hour, unless meteorological conditions are ideal.

Figure C5 shows comparisons among the three collocated sensors under an easterly wind regime, with the data averaged in 5 minute blocks. Note that the calculated horizontal wind speeds differ by 1 m/s or less among sensors.

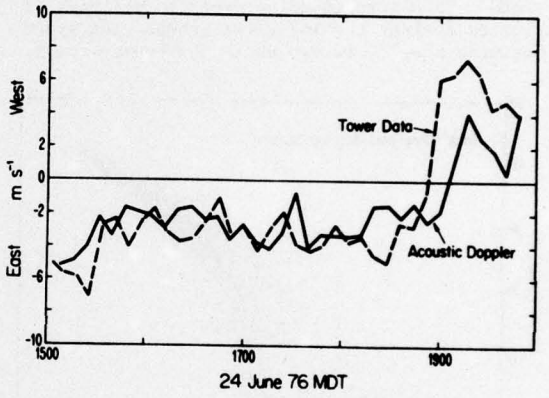

Figure C4. Comparison of horizontal wind speeds (east-west component) between acoustic Doppler and tower (approx. 2 km separation). 8 min block averages of east-west components were plotted. Altitude was about 150 m AGL.

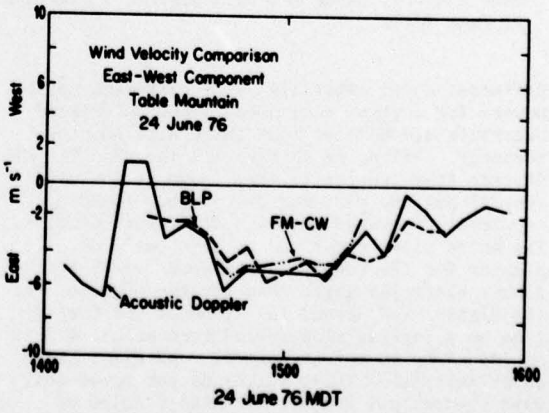

Figure C5. Comparison of horizontal wind estimates from acoustic Doppler, FM-CW radar and BLP tethered balloon. 5 min block averages of east-west components were plotted. Altitude was about 210 m AGL.

PERFORMANCE UNDER EXTREME CONDITIONS

The limiting factor in the current acoustic Doppler system appears to be audible noise. Noise has been classified as near field (from wind, rain, birds, and insects) and far field (from traffic, thunder and turbulence). The near-field noise, particularly that generated by wind or rain on the bunker cover, is a category over which we have some limited design control. Empirical selection of the best cover material is a goal of the Table Mountain tests. Cover materials installed so far have been different types of acoustically transparent foam or matting.

Wind-generated noise often occurs without other adverse phenomena and is a function of wind speed. In Figure C6 noise power in decibels is plotted against the logarithm ground wind speed, measured about 2 meters above the bunker cover.

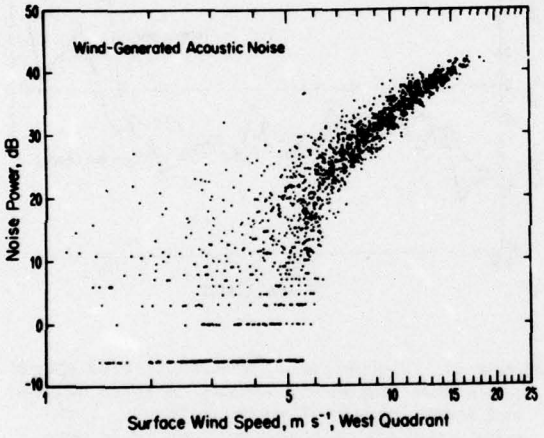

Figure C6. Noise power as a function of westerly surface wind speed on logarithmic plot. Data were taken at Table Mountain between 8 June and 21 June 1976.

Different cover materials yield different noise powers for a given wind speed. Rough-surfaced materials are noisier than those with smoother textures. All noise sources are included in this diagram (the scatter is very large at low wind speeds) but the wind noise at higher speeds completely overshadows noise from other sources. The noise power was found to be about 3 dB greater for the receiver transducer aimed at the lowest elevation angle than for the highest. At the higher wind speeds the slope of the best-fit line on a log-log plot varied from about +4.5 to +8 depending on meteorological conditions and cover material. These values do not agree well with theoretical and experimental studies of noise generated by wind blowing over rough surfaces, which indicate a 4th power relationship. Thus, there may be an additional source of noise under windy or highly turbulent conditions, beyond that generated directly on bunker cover material by the wind. This noise could be generated aerodynamically in the turbulent flow itself.

This phase of the tests also has shown that the noise power due to wind blowing directly into the bunker is about 3 dB greater than that from wind blowing from behind the bunker. Rain-generated noise has been found to be less severe than that from other sources. In fact, during thunderstorm conditions, it is difficult, with the data collected so far, to separate the amount of degradation due to rain noise from that due to other limiting factors. It was observed on several occasions when heavy precipitation commenced abruptly, that system outage did not occur for several minutes. A wind profile measured during intense rain (about 13 cm hr^{-1}) shows reliable operation up to 400 meters. It was hypothesized that the noise of water dripping inside the bunker, which starts after cover saturation, is the primary cause of system degradation during rain. Bunker design improvements were then made to substantially reduce the dripping, but nature has not since provided appropriate heavy rain conditions. Thus, no reasonable rain limitation figures can yet be assigned to the Table Mountain system.

PERFORMANCE UNDER AVERAGE CONDITIONS

In order to summarize the field operating reliability of the acoustic Doppler system, one must include the combined effects of many degrading factors: noise from various sources, inexact beam alignment for particular wind conditions, and the lack of acoustic scatterers. Since wind noise appears to be the primary cause of limiting conditions at Table Mountain, scatter diagrams were constructed to present system reliability as a function of wind speed. Figure C7 summarizes a collection of diagrams from different days. Performance is shown for three

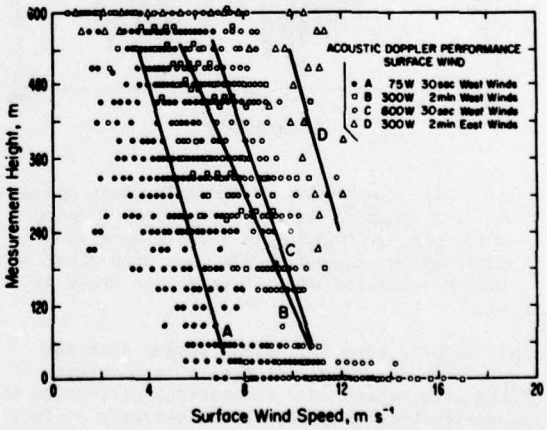

Figure C7. Height of highest reliable measurement (system reliability of 75%) as a function of surface wind speed. A) westerly winds, 30 sec system data averaging, 75 W main transmitter power. B) Westerly winds, 2 min averaging, 300 W. C) Westerly winds, 30 sec averaging, 600 W. D) Easterly winds, 2 min averaging, 300 W.

power settings. The horizontal axis is wind speed and the vertical axis is the height of the highest gate at which a 75% or greater reliability was achieved. System reliability figure is determined by self-diagnosis of signal-to-noise ratio, overload, and minimum signal criteria failure rates. (A 75% to 80% minimum system reliability figure for the Table Mountain system is based on extensive real-time observations and post analysis of events for internal consistency and continuity.) It is evident that under westerly surface wind conditions (worst case, with wind blowing down the bunker throat) good performance cannot be expected with surface winds much above 10 m/s. Increased system reliability can be obtained with longer averaging times since each average contains more samples of the wind. The improvement in performance can be seen in Figure C7 by comparing curves B and C. Although the transmitted power has been decreased by a factor of two from C to B, increasing the averaging time from 30 s to two minutes resulted in little performance change at low altitudes. Note that these figures also include the effects of variability of acoustic scatterers and the effect of wind blowing the transmitted/scattered acoustic beams away from the maximum lobe in the receiver beam pattern.

The cause of system outage from wind noise is more complex than the one-to-one relationship suggested above. Reliable wind measurements over 400 meters have been obtained with ground wind averaging about 15 m s^{-1}. These situations may have been blessed with extremely strong acoustic scattering. From several cases examined, there seems to be greater scattering and/or less noise during wind-shear events than during high wind situations when the boundary layer is well mixed.

Overall, the system operates reliably (with a system reliability figure of 0.75) most of the time up to 300 m, about 75% of the time up to 400 m and about 40% of the time up to 600 m.

Note also that the rapid degradation with increasing wind speed starts at a speed of about 6 m s^{-1}. This speed corresponds to the onset of significant wind-generated noise (see Figure C6). Speeds below about 6 m s^{-1} produce noise which is not significantly higher than other noise sources (traffic, insects, birds, etc.).

By plotting a number of these reliability versus wind speed scatter diagrams at various transmitter power settings (Figure C7), one can assess the improvement in system reliability that can be obtained by increasing the transmitted acoustic power under windy conditions at the surface. The Table Mountain system at 300 m can reliably tolerate an increase in surface wind speed from 5 to 9 m s^{-1} by increasing the transmitted power from 75 to 600 W. However, atmospheric variability from day to day often obscured this simple formula, and occasions were discovered when the system would perform at nearly its best with much less power than 600 W. As noted earlier, strong easterly winds degrade the system less than strong westerly winds do.

Since a small increase in wind speed yields a great increase in noise power, merely doubling or quadrupling the transmitter power will not result in a comparable increase in performance.

The archived data were also investigated to answer questions about the availability of acoustic scatterers. The most direct approach seemed to be to look at the temporal variations in received signal power. An estimate of the signal power at any height was obtained by integrating the received power spectra, corresponding to that height, over a narrow band 50 Hz wide, centered on the Doppler-shifted signal peak. Besides variations in the scattering parameters of interest (C_v^2, C_T^2), fluctuations in the signal power estimates can be due to temporal variations in attenuation along the path of the beam, in ray bending, in translation of the beam by the wind across the receiver beam pattern, and in noise power in the narrow band. A sample time series of this received signal power estimate is shown in Figure C8. Note that the received power from 600 m is typically 18 dB less than that from 210 m.

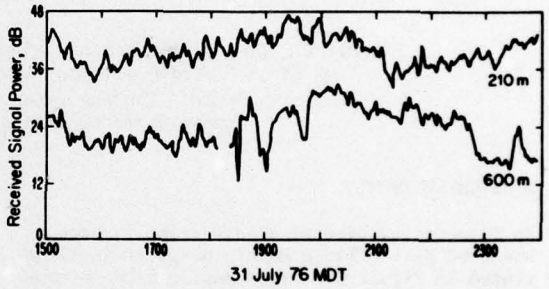

Figure C8. Temporal variation of received signal power for two heights (210 m, 600 m). System averaging time constant was 2 min.

From several sets of time series for several altitudes, some general statements can be made about variations in received signal power. The narrow-band power decreases by as much as 30 dB at a height of 210 m from day time to nightime. Sometimes the changes are abrupt steps which correlate with abrupt changes in the wind speed/direction on the ground as well as aloft. Short-term fluctuation in received power by this method appears to be about 6 dB. Furthermore, the variation in signal power at high gates is much greater than near the surface. Received power decreases aloft but not in a simple manner and there appears to be more power received during periods of easterly winds than westerly winds.

The wind measurement accuracy of the atmospheric heights serviced by the satellite transmitter has been a subject of some concern also. For the two-week test period long time series of wind speed were plotted for altitudes immediately above and below the satellite-main transmitter cross-over. Though the series cannot be expected to be extremely similar, no gross differences were seen among all the main and satellite gates inspected. The satellite volume is separated from the main transmitter volume by more than 250 meters.

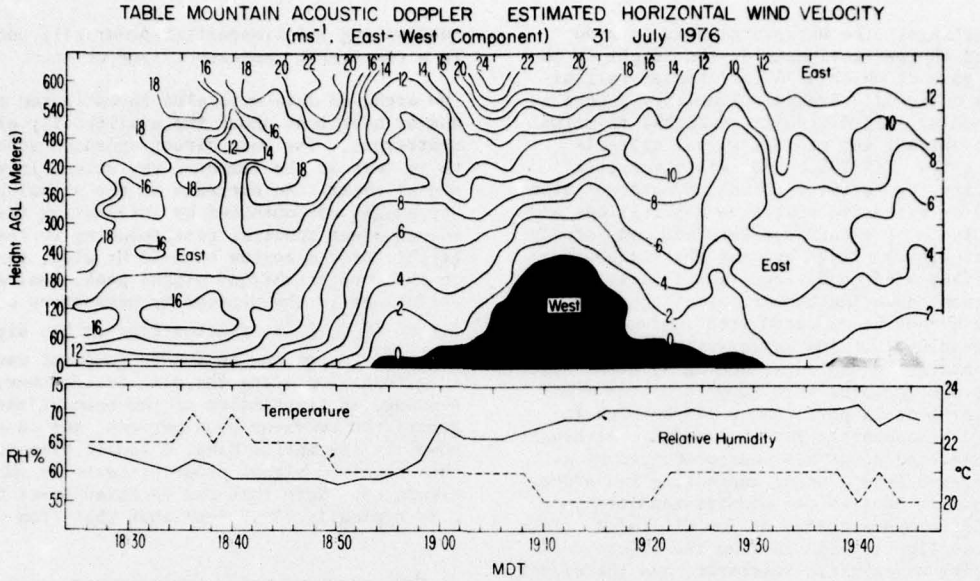

Figure C9. Time-height section of estimated east-west horizontal wind velocity from Table Mountain acoustic Doppler system on 31 July 1976. Westerly winds are shaded. Contour intervals are 2 m s^{-1}; surface temperature and relative humidity time series are shown at the bottom.

WIND-SHEAR EVENT

An interesting case of a gust-front passage as measured by the Table Mountain system is illustrated in Figure C9. This depiction describes part of the thunderstorm development on 31 July 76 which preceeded the Big Thompson flood. Some of the strongest low-level easterly winds ever detected in Eastern Colorado occurred on this day. As the site was unattended, no specifics can be given regarding the thunderstorm cell pattern surrounding Table Mountain. It seems reasonable, however, that the cell(s) which produced the observed downdraft was somewhere to the west of the site, at least a few kilometers distant.

Fairly strong easterly winds eventually gave way to a good vertical E-W speed shear as the low-level winds dropped off. Intrusion of low-level westerly flow is seen about 1/2 of the way through the sequence. It is interesting to note that the wind-shear value measured at the strongest point is almost as great as that inferred during the DC-10 crash at Boston in 1973. The shear value seen here is only one component and reaches nearly 25 m/s over the 600 meter depth. Eventually the strong easterly component returns throughout the profile.

CONCLUSION

System Performance

The primary limiting factor in the current prototype acoustic Doppler system is audible noise. The exact causes of system degradation appear to be more complicated than one would expect; more complex and interesting than just wind or rain noise or other easily classifiable parameter. Very good results have been obtained, on occasion, with strong surface wind and heavy rain. Poor results have been observed under apparently favorable conditions. The distribution or climatology of acoustic scattering is an important aspect which has not been fully investigated. Under most circumstances, the maximum westerly surface wind under which the Table Mountain system can operate is about 10 m/s. This figure may be raised only slightly by "fine tuning" the current design or significantly by improving both hardware and software design.

Wind Measurement Accuracy

Within the experimental and atmospheric limitations previously described, the acoustic Doppler system seems to measure the horizontal wind speed to within its design criterion of 1 m s^{-1}. The time averaging of data needed to establish this conclusion is justified under the condition of synoptic-scale wind shear measurements. Vertical motions measured by the sounder significantly affect the estimate of horizontal winds, especially at the higher levels; it is recommended that raw estimates be averaged for 10 minutes. Whether the system accurately measures the wind fluctuations down to its small-scale limit, and the establishment of this limit, are questions of significant research interest but have not yet been pursued.